CENTRO DE INVESTIGACIONES
EN ÓPTICA, A.C.

“Diffractive and non-diffractive beams and pulses; a comparative study ”

Thesis submitted in fulfillment of the requirements for the master degree in science (Optics)

Physicist Etna Dafne Yáñez Roldán

Advisor: Dr. Moisés Cywiak Garbarcewicz

July 2016

León Guanajuato, México

"Finally we ought to employ all the aids of understanding, imagination, sense and memory, first for the purpose of having a distinct intuition of simple propositions; partly also in order to compare the propositions to be proved with those we know already, so that we may be able to recognize their truth; partly also in order to discover the truths, which should be compared with each other so that nothing may be left lacking on which human industry may exercise itself".

René Descartes

Gratefulness

All my gratitude to *God,* who is my refuge and strength, and my ever-present help in trouble.

I want to thank Luis and Neizan for all their precious support and kindness, without them it couldn´t be possible to achieve this goal.

I want to thank my family for being there always in bad and good times, they impulse me to be a better person, I love them.

Special thanks to Dr. Moisés Cywiak for his wisdom advices, his endeavor, patience and time, to Mary for being gentile, to my friend Franco for his special sense of humor and enormous help and to Moi for his explanations and genuine friendship.

To my reviewers: Dr. David Moreno and Dr. Mauricio Flores for their well-aimed suggestions and for all their support along my master.

To Hugo, Adrián and Ángeles who always were available for helping me and also thanks to all the personnel at CIO.

And special thanks to CONACyT for financial support.

Table of Contents

Abstract

Analytical methods are described which allow us to perform a comparative study of diffractive and non-diffractive beams and pulses. Our description first reviews basic properties of the Fresnel diffraction integral applied for calculating the propagation of well-known beams. Then, different methods to obtain exact solutions to the wave equation in free space are described and their diffractive properties are analyzed. The methods described generate solutions which represent pulses or beams spatially localized and also pulses or beams that spatially propagate exhibiting spreading or diffraction, in a similar way as typical diffractive beams. Additionally, some of the solutions represent localized superluminal pulses. Computer simulations are provided to allow a comprehensive comparison of the performance of the diffractive and non-diffractive solutions.

Chapter 1

Introduction

Diffraction is an optical phenomenon that produces spatial broadening of a beam or a pulse while it travels or propagates in free space. Although in general, some benefits can be obtained from the diffractive properties of beams and pulses, there are a lot of applications in which keeping the transverse size of a light beam would be of benefit as in the case of biomedical images or space communications [1]. In some cases then, spreading or widening of beams due to diffraction result as a limiting factor to achieve high quality images or information. Then, developing beams or pulses without (or less) diffraction and dispersion is important to several applications [1-2].

Basically, the differential equation in free space is the starting point to obtain non-diffractive or localized solutions. These solutions are also denominated **Focus Wave Modes**. Solutions to the wave equations in this sense were developed years ago [3-9] and since then extensive research has been conducted on the subject to obtain new solutions. Additionally, experimental research has also been performed to attain physically these beams and pulses [10-13].

The first experimental observation of a moving pulse that travels without distortion and that reproduces its initial shape at certain distances was observed by J. Scott in August 1834 and was called a **soliton** [14]. Later, James Neill Brittingham demonstrated that a soliton-like solution satisfied the homogeneous wave equation; but the soliton carries infinite energy [3]. After this, Sezginer [15] obtained a truncated wave, soliton-like solution with finite energy. In 1985 Ziolkowski proposed a solution to the wave equation which propagated without deformation within a limited distance of propagation in free space carrying finite energy; these experiments were conducted using acoustic waves [4, 10-13].

Using a different approach, in 1987 J. Durnin discovered independently a new localized wave solution [7]. This solution was expressed as a continuous Bessel beam [16,17]. Further experiments were performed using this solution [8, 17-19]. However, again, the Bessel non-diffractive beam carries infinite energy and to be physically realizable this wave requires truncation. As a consequence, when properly truncated, its non-diffractive behavior is maintained only on a limited distance of propagation [13, 18-20]. These truncated beams are referred as localized beams with a large depth of field [19-20]. There are several techniques to experimentally achieve the Bessel beams, interferometric [21-22], using conical lenses or axicons [23-25] and producing energy pulse trains as proposed by Ziolkowski [10] using ultrasonic waves in water. The first acoustical Bessel beam generator was reported by Hsu [26].

It is important to remark that the first J_0 Bessel non-diffracting optical beam was obtained by Durnin using an annular aperture. Looking for new solutions, Jian-yu Lu and J. Greenleaf in 1992 described a manner to obtain the now known X-waves [9-11]. Other solutions have been developed since then [27].

In this thesis we provide a detailed mathematical analysis for obtaining exact solutions to the differential equation in free space. Some of the solutions will result in localized wave solutions, non-diffractive beams and pulses, other solutions will result in well-known diffractive beams.

Our description is presented in chapters as indicted in the index. We begin in the next chapter with a brief description of some useful properties of the Fourier transform that will allow us to introduce in the following chapters mathematical tools required for calculating analytically the Fresnel propagation that will be used for comparative purposes.

Chapter 2

Fourier Analysis

In this chapter we review some concepts of the Fourier transform to be used in diffractive pattern calculations. For illustrative purposes some examples are included.

2.1 The Fourier Transform

The Fourier transform in the space function, for an arbitrary function $f(x,y)$, complex in general, is defined as

$$\mathcal{F}\{f(x,y)\} = F(u,v) = \int_{-\infty}^{\infty}\int_{-\infty}^{\infty} f(x,y)e^{-i2\pi(ux+vy)}\,dxdy\,, \tag{2.1}$$

where $F(u,v)$ is the function in the frequencies space and (u,v) are the spectral coordinates for (x,y) respectively. It is possible to calculate the inverse Fourier transform as,

$$\mathcal{F}^{-1}\{F(u,v)\} = f(x,y) = \int_{-\infty}^{\infty}\int_{-\infty}^{\infty} F(u,v)e^{i2\pi(ux+vy)}\,dudv, \tag{2.2}$$

2.2 Some properties of the Fourier Transform.

We now consider a few of the basic mathematical properties of the Fourier transform [28], that will be used in following chapters.

• Linearity: The transform of a weighted sum of two or more functions is simply the identically weighted sum of their individual transforms

$$\mathcal{F}\{ag + bh\} = a\mathcal{F}\{g\} + b\mathcal{F}\{h\} = aG(u) + bH(u), \tag{2.3}$$

• Multiplication

$$\mathcal{F}\{g \cdot h\} = G(u) \otimes \mathrm{H(u)}, \tag{2.4}$$

where we define the convolution $\otimes$ as

$$G(u,v) \otimes \mathrm{H(u,v)} = \iint_{-\infty}^{\infty} g(x,y)h(u-x,v-y)dxdy\,. \tag{2.5}$$

• Convolution: if $\mathcal{F}\{g(x,y)\} = G(u,v)$ and $\mathcal{F}\{h(x,y)\} = H(u,v)$, then

$$\mathcal{F}\{g(x,y) \otimes h(x,y)\} = G(u,v) \cdot H(u,v)\,, \tag{2.6}$$

the convolution of two functions in the space domain (an operation that will be found to arise frequently in the theory of linear systems) is entirely equivalent to the more simple operation of multiplying their individual transforms and inverse transforming.

• Scaling: if $\mathcal{F}\{g(x,y)\} = G(u,v)$ then,

$$\mathcal{F}\{g(ax,by)\} = \frac{1}{|ab|} G\left(\frac{u}{a},\frac{v}{b}\right)\,, \tag{2.7}$$

that is, a stretch of the coordinates in the space domain (x,y) results in a contraction of the coordinates in the frequency domain (u,v), plus a change in the overall amplitude of the spectrum.

• Shift theorem: if $\mathcal{F}\{f(x,y)\} = F(u,v)$ then,

$$\mathcal{F}\,\{f(x-x_0,y-y_0)\} = e^{-i2\pi(ux_0+vy_0)}F(u,v)\,, \tag{2.8}$$

that is, a translation in the space domain introduces a linear phase shift in the frequency domain.

• Parseval´s theorem (Rayleigh's theorem): if $\mathcal{F}\{g(x,y)\} = G(u,v)$ then,

$$\int_{-\infty}^{\infty}\int_{-\infty}^{\infty}|g(x,y)|^2dxdy = \int_{-\infty}^{\infty}\int_{-\infty}^{\infty}|G(u,v)|^2du\,dv\,, \tag{2.9}$$

the integral on the left-hand side of this theorem can be interpreted as the energy contained in the waveform $|g(x,y)|^2$. This in turn leads us to the idea that the quantity $|G(u,v)|^2$ can be interpreted as an energy density in the frequency domain.

- Fourier integral theorem: At each point of continuity of g,

$$\mathcal{F}\mathcal{F}^{-1}\{g(x,y)\} = G^{-1}G(u,v) = g(x,y)\ , \tag{2.10}$$

at each point of discontinuity of g, the two successive transforms yield the angular average of the values of g in a small neighborhood of that point. That is, the successive transformation and inverse transformation of a function yields that function again, except at points of discontinuity.

2.3 Fourier transform of a Gaussian distribution

In a following chapter we will require the Fourier transform of a Gaussian function. We introduce a Gaussian function in the form $f(x) = e^{-\pi x^2}$. Its Fourier transform is given by

$$\mathcal{F}\{f(x)\} = \mathcal{F}\left\{e^{-\pi x^2}\right\} = F(u) = \int_{-\infty}^{\infty} e^{-\pi x^2} e^{-i2\pi ux} dx\ , \tag{2.11}$$

performing the integral, we obtain,

$$\mathcal{F}\left\{e^{-\pi x^2}\right\} = F(u) = e^{-\pi u^2}. \tag{2.12}$$

Using the scaling property, we obtain the following useful expression,

$$\mathcal{F}\left\{e^{-\pi(ax)^2}\right\} = \frac{1}{a} e^{-\pi\left(\frac{u}{a}\right)^2}\ . \tag{2.13}$$

in an specific case where $a = \frac{1}{\sqrt{\pi}\cdot r_0}$

$$\mathcal{F}\left\{e^{-\pi\left(\frac{x}{\sqrt{\pi}\cdot r_0}\right)^2}\right\} = \mathcal{F}\left\{e^{-\left(\frac{x}{r_0}\right)^2}\right\} = \sqrt{\pi} r_0 e^{-(\pi r_0 u)^2}. \tag{2.14}$$

The above result indicates that the Fourier Transform of a Gaussian spatial function is also a Gaussian function in the frequency space. Figure 2.1 shows normalized amplitudes of the Gaussian distribution in the spatial domain and in its corresponding spectral space.

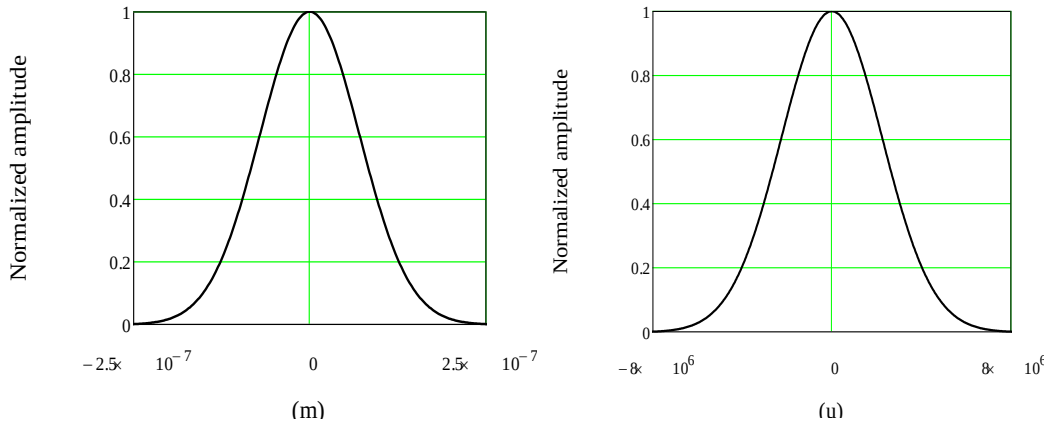

Figure 2.1. a) Normalized Gaussian function in its space domain and b) its normalized Fourier transform (frequency domain) where the units of u are m^{-1}. for $r_0 = 0.1 \times 10^{-6}\ \mathrm{m}$.

2.4 Functions with Circular Symmetry: Fourier-Bessel Transforms

A function g is said to be circularly symmetric or axisymmetric if it can be written as a function of the radius ρ alone, that is,

$$g(\rho, \emptyset) = g(\rho)\ . \tag{2.15}$$

The Fourier transform of g in a system of rectangular coordinates is given by

$$\mathcal{F}\{g(x,y)\} = G(u,v) = \int_{-\infty}^{\infty}\int_{-\infty}^{\infty} g(x,y)e^{-i2\pi(ux+vy)}\,dxdy\ , \tag{2.16}$$

we can make a transformation to polar coordinates in both (x, y) and (u, v) planes as follows

$$x = \rho \cos \emptyset \ , \qquad y = \rho \sin \emptyset \ , \tag{2.17}$$

$$u = r \cos \Theta \ , \qquad v = r \sin \Theta \ , \tag{2.18}$$

$$\rho = \sqrt{x^2 + y^2} \ , \quad r = \sqrt{u^2 + v^2} \ , \tag{2.19}$$

and the Fourier transform may be rewritten as

$$G(r, \Theta) = \int_0^\infty g(\rho) \, \rho d\rho \int_0^{2\pi} e^{-i2\pi r\rho \cos(\emptyset - \Theta)} d\emptyset \ , \tag{2.20}$$

finally, we use the Bessel function identity

$$J_0(a) = \frac{1}{2\pi} \int_0^{2\pi} e^{-ia \cos(\emptyset - \Theta)} d\emptyset \ , \tag{2.21}$$

where J_0 is a Bessel function of the first kind, zero-order.

Thus the Fourier transform of a circularly symmetric function (with dependence only of radius) is itself circularly symmetric and can be found as

$$G(r, \Theta) = G(r) = 2\pi \int_0^\infty g(\rho) \, J_0(2\pi r\rho) \rho d\rho \ . \tag{2.22}$$

As demonstrated by the above equation a function which is circularly symmetric in the ρ space results also circularly symmetric in its corresponding spectral space. This is an important property that will be used in the next chapter.

Chapter 3

Analytical calculation of diffraction fields

In this chapter we present some analytical properties of the propagation of beams.

3.1 Fresnel Diffraction Integral

To calculate the propagation of fields in the paraxial region the most useful analytical tool is the Fresnel diffraction integral [29-31]. This integral has demonstrated that although it is an approximation and it does not satisfy the wave equation in the free space gives accurate results that properly match with experimental observations. It has to be remarked that its validity begins for distances of a few wavelengths up to far fields from the object plane; however, as indicated, the diffraction patterns obtained with the Fresnel diffraction integral represent accurately experimental measurements.

The Fresnel diffraction integral is defined as

$$\Psi_F(\xi,\eta) = \frac{e^{ikz}}{\sqrt{i\lambda z}} \iint_{-\infty}^{\infty} \Psi_I(x,y)\, e^{i\frac{\pi}{\lambda z}[(x-\xi)^2+(y-\eta)^2]} dxdy\,, \tag{3.1}$$

where $i=\sqrt{-1}$, and λ is the wavelength of the source field and the indexes F and I are for final and initial fields.

Figure 3.1 illustrates the physical situation for applying the Fresnel diffraction integral. The object plane is located in a coordinate plane $(x,y,z=0)$. The plane of observation is located in a coordinate plane $(\xi,\eta,z=z)$.Both planes are parallel and are at a distance z .

By expanding the quadratic terms in the Fresnel integral allows writing equation (3.1) as

$$\Psi_F(\xi,\eta) = \frac{e^{ikz}}{\sqrt{i\lambda z}} e^{i\frac{\pi}{\lambda z}(\xi^2+\eta^2)} \iint_{-\infty}^{\infty} \Psi_I(x,y)\, e^{i\frac{\pi}{\lambda z}(x^2+y^2)} e^{-i\frac{2\pi}{\lambda z}(x\xi+y\eta)} dxdy\,, \tag{3.2}$$

which, by using the Fourier transform notation can be written compactly as,

$$\Psi_F(\xi,\eta) = \frac{e^{ikz}}{\sqrt{i\lambda z}} e^{i\frac{\pi}{\lambda z}(\xi^2+\eta^2)} \mathcal{F}\left\{\Psi_I(x,y) e^{i\frac{\pi}{\lambda z}(x^2+y^2)}\right\}. \tag{3.3}$$

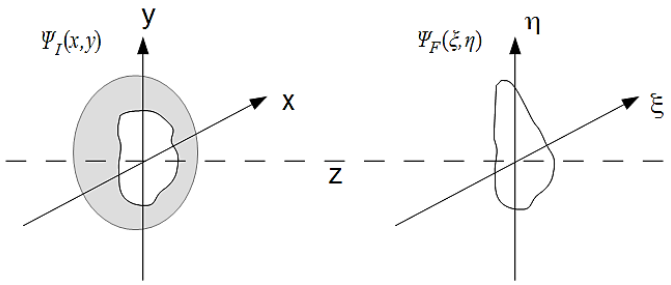

Figure 3.1. Amplitude distribution $\Psi_I(x,y)$ at a plane $(x,y,z=0)$ and its corresponding distribution $\Psi_F(\xi,\eta)$ in a plane of observation $(\xi,\eta,z=z)$ after propagating a distance *z*.

As indicated, equation (3.3) represents a compact form of the Fresnel diffraction integral. Using properties described in chapter 2 inherently implies calculating a convolution in the Fourier space. This result will find to be useful in following chapters.

3.2 The Fraunhofer approximation

In the previous section we emphasized that the amplitude distribution in the observation plane inherently involved the convolution of the spectral functions of the object distribution with a quadratic phase term. For some applications it will be convenient to circumvent the presence of the quadratic phase term. This can be accomplished by moving away the plane of observation at a far distance such that

$$z \gg \frac{k(x^2+y^2)}{2}. \tag{3.4}$$

When this approximation is valid the intensity distribution results approximately the one that corresponds to the Fourier transform of the object amplitude distribution

[29-31]. Under this condition these calculations are known as the Fraunhofer propagation, and can be written as

$$\Psi_F(\xi,\eta) = \frac{e^{ikz}}{\sqrt{i\lambda z}} e^{i\frac{\pi}{\lambda z}(\xi^2+\eta^2)} \mathcal{F}\{\Psi_I(x,y)\}\,. \tag{3.5}$$

In equation (3.5) the quadratic phase has been neglected. Equation (3.5) explicitly establishes that in the Fraunhofer regime the amplitude distribution at a far plane of observation consists of a quadratic phase term multiplied by the Fourier transform of the amplitude distribution at the object plane.

In the next section will show examples of one-dimensional functions and distributions.

3.3 Some examples of the Fresnel propagation.

3.3.1 Example 1: Propagation of a Gaussian distribution (one dimension)

For brevity we will address to a one-dimensional Gaussian distribution without loss of generality. The amplitude distribution at the object plane with semi-width r_0, can be written as

$$\Psi(x) = e^{-\left(\frac{x}{r_0}\right)^2}. \tag{3.6}$$

Substituting this equation in the Fresnel integral (3.1) gives,

$$\Psi(\xi) = \frac{e^{ikz}}{\sqrt{i\lambda z}} \int_{-\infty}^{\infty} e^{-\frac{x^2}{{r_0}^2}} e^{i\frac{\pi}{\lambda z}(x-\xi)^2} dx\,. \tag{3.7}$$

This integral can be solved analytically as follows. First we expand the quadratic phase as,

$$\Psi(\xi) = \frac{e^{ikz}}{\sqrt{i\lambda z}} e^{i\frac{\pi}{\lambda z}\xi^2} \int_{-\infty}^{\infty} e^{-\pi x^2\left(\frac{\lambda z - i\pi}{\pi {r_0}^2} - \frac{i}{\lambda z}\right)} e^{i\frac{2\pi}{\lambda z}x\xi} dx. \tag{3.8}$$

Now, we introduce the new parameter $u = \frac{\pi}{\lambda z}$ to obtain,

$$\Psi(\xi) = \frac{e^{ikz}}{\sqrt{i\lambda z}} e^{i\frac{\pi}{\lambda z}\xi^2} \mathcal{F}\left\{ e^{-\pi x^2\left(\frac{\lambda z - i\pi {r_0}^2}{\pi {r_0}^2 \lambda z}\right)} \right\}\Big|_{u=\frac{\xi}{\lambda z}} , \tag{3.9}$$

using the Fourier transform properties of chapter 2, we can finally rewrite equation (3.9) as,

$$\Psi(\xi) = \frac{e^{ikz}}{\sqrt{i\lambda z}} \cdot \sqrt{\frac{\pi {r_0}^2 \lambda z}{\lambda z - i\pi {r_0}^2}} \cdot e^{i\frac{\pi}{\lambda z}\xi^2} e^{-\pi\left(\frac{\pi {r_0}^2 \lambda z}{\lambda z - i\pi {r_0}^2}\right)\left(\frac{\xi}{\lambda z}\right)^2} . \tag{3.10}$$

To visualize the meaning of equation (3.10), we rewrite it as,

$$\Psi(\xi) = \frac{e^{ikz}}{\sqrt{i\lambda z}} \cdot \sqrt{\frac{\pi {r_0}^2 \lambda z}{\lambda z - i\pi {r_0}^2}} e^{i\frac{\pi}{\lambda z}\xi^2} e^{-\pi^2 {r_0}^2\left(\frac{\lambda z + i\pi {r_0}^2}{\lambda^2 z^2 + \pi^2 {r_0}^4}\right)\frac{\xi^2}{\lambda z}} . \tag{3.11}$$

It will be noticed that equation (3.11) represents a Gaussian distribution with a quadratic phase. It can be compactly be written as,

$$\Psi(\xi) = \frac{e^{ikz}}{\sqrt{i\lambda z}} \cdot \sqrt{\frac{\pi {r_0}^2 \lambda z}{\lambda z - i\pi {r_0}^2}} \cdot e^{-\frac{\xi^2}{r^2}} e^{i\frac{\pi\xi^2}{\lambda R}} , \tag{3.12}$$

where we define the complex constant term as,

$$A = \frac{e^{ikz}}{\sqrt{i\lambda z}} \cdot \sqrt{\frac{\pi {r_0}^2 \lambda z}{\lambda z - i\pi {r_0}^2}} , \tag{3.13}$$

r is the semi-width of the Gaussian beam,

$$r = r_0 \sqrt{1 + \frac{\lambda^2 z^2}{\pi^2 {r_0}^4}} , \tag{3.14}$$

and R is the radius of curvature,

$$R = \frac{\lambda^2 z^2 + \pi^2 {r_0}^4}{\lambda^2 z} . \tag{3.15}$$

It can be noticed in the above equation that there are two terms that correspond to the amplitude and to the radial distribution of the Gaussian beam at the plane of observation. As the distance of propagation z increases then the semi-width of the beam becomes wider while its amplitude decreases; this is a necessary condition because the energy of the beam must be conserved. The last term of equation 3.12 represents a quadratic phase similarly to a spherical wave. Figure 3.2 shows how the Gaussian beam intensity distribution evolves as it propagates along the z distance.

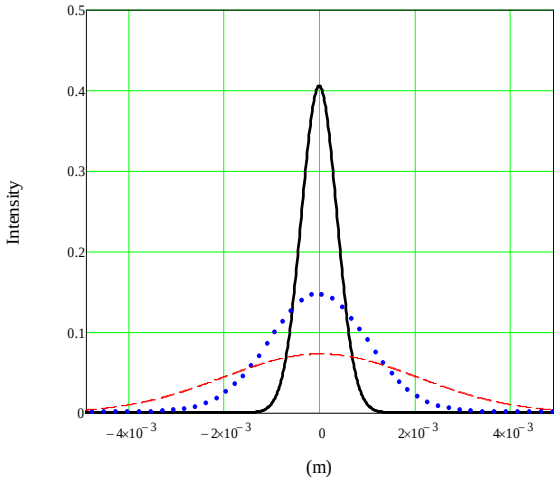

Figure 3.2 . Gaussian intensity distributions at three distances of propagation. The continuous line plot is at $z = 1$ m, the dotted line plot is at $z = 3$ m and the dashed line plot is at $z = 6$ m, $r_0 = 6 \times 10^{-4}$ m and $\lambda = 638 \times 10^{-9}$ m.

3.3.2 Example 2: Propagation of a Circ function.

The Circ function is defined as

$$\mathrm{Circ(r)} = \begin{cases} 1 & \text{if} \quad \mathrm{r} < a \\ 0 & \text{otherwise} \end{cases}, \tag{3.16}$$

where

$$\mathrm{r} = \sqrt{x^2 + y^2}, \tag{3.17}$$

and a represents the radius of the circular aperture.

The corresponding amplitude distribution in the plane $(\xi - \eta)$ can be calculated by means of the Fresnel integral,

$$\Psi(\xi,\eta) = \frac{e^{ikz}}{\sqrt{i\lambda z}} \iint_{-\infty}^{\infty} \Psi(x,y)\, e^{i\frac{\pi}{\lambda z}[(x-\xi)^2+(y-\eta)^2]} dxdy\,. \qquad (3.18)$$

For solving the above integral it will be convenient to introduce the following change of variables,

$$x = \rho\cos\emptyset\,,\ y = \rho\sin\emptyset, \qquad (3.19)$$

$$\xi = r\cos\Theta\,,\ \eta = r\sin\Theta. \qquad (3.20)$$

It will be noticed that by substituting the Circ function in $\Psi(x,y)$ in equation (3.18), the object function $\Psi(x,y)$ will now be a function of the form $\Psi(\rho,\phi)$. Furthermore, being a symmetrical function in ϕ it can finally be written as a function of only one variable as $\Psi(\rho)$.

Under the above conditions, equation (3.18) can now be written as,

$$\Psi(\xi,\eta) = \frac{e^{ikz}}{i\lambda z} e^{i\frac{\pi}{\lambda z}r^2} \int_0^{\infty} \Psi(\rho) d\rho\ \rho e^{i\frac{\pi}{\lambda z}\rho^2} \int_0^{2\pi} \mathrm{d}\emptyset\, e^{-i\frac{2\pi}{\lambda z}r\rho\cos(\emptyset-\Theta)}\,. \qquad (3.21)$$

To proceed further we use the integral definition of the Bessel function of the first kind, zero-order (2.21) to obtain,

$$\Psi(\xi,\eta) = \frac{e^{ikz}}{i\lambda z} e^{i\frac{\pi}{\lambda z}r^2} 2\pi \int_0^{\infty} \Psi(\rho) e^{i\frac{\pi}{\lambda z}\rho^2} \mathrm{J}_0\left(\frac{2\pi}{\lambda z}r\rho\right)\rho\, d\rho\,. \qquad (3.22)$$

The integral in equation (3.22) cannot be solved in a closed form and it has to be estimated by numerical algorithms. However, for illustrative purposes we will limit ourselves to calculate this integral using the Fraunhofer approximation. Thus, for this case, we can neglect the term $e^{i\frac{\pi}{\lambda z}\rho^2}$ and write the integral in (3.22) as,

$$\Psi(\xi,\eta) = \frac{e^{ikz}}{i\lambda z} e^{i\frac{\pi}{\lambda z}r^2} 2\pi \int_{\rho=0}^{\rho=a} \Psi(\rho)\, \mathrm{J}_0\left(\frac{2\pi}{\lambda z}r\rho\right)\rho\, d\rho\,. \qquad (3.23)$$

Now, to solve the integral in the above equation we make the following change of variables

$$s = \frac{2\pi}{\lambda z} r\rho, \qquad \frac{\lambda}{2\pi r} ds = d\rho. \tag{3.24}$$

Equation (3.23) without considering multiplicative factor can now be written as,

$$\Psi(r) = \left(\frac{\lambda z}{2\pi r}\right)^2 \int_{s=0}^{s=\frac{2\pi}{\lambda z} ra} s\, \mathrm{J}_0(s) ds\,. \tag{3.25}$$

Using the following property,

$$\int_0^b x\, \mathrm{J}_0(\mathrm{x}) dx = x J_1(x)|_0^b\,, \tag{3.26}$$

leads to,

$$\Psi(r) = a^2 \frac{J_1\left(\frac{2\pi}{\lambda z} ra\right)}{\left(\frac{2\pi}{\lambda z} ra\right)}. \tag{3.27}$$

Using the definition of the Bessel-sinc, $\mathrm{Bsinc}(x)$ function, $\mathrm{Bsinc}(x) = \frac{J_1(x)}{x}$, allow us to write finally equation (3.27) as

$$\Psi(r) = a^2 \mathrm{Bsinc}\left(\frac{2\pi}{\lambda z} ra\right). \tag{3.28}$$

A plot of the above equation is shown in figure 3.3.

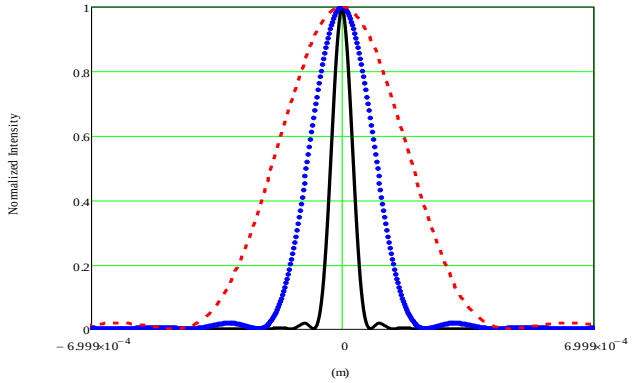

Figure 3.3. Bsinc intensity distributions in the plane of observation. The continuous line plot is at $z = 1$ m, the dotted line plot is at $z = 3$ m and the dashed line plot is at $z = 6$ m, with $a = 5 \times 10^{-3}$ m and $\lambda = 638 \times 10^{-9}$ m.

3.3.3 Example 3: Far propagation of an annular slit

In this example we describe how to generate a Bessel function of the first kind zero-order due to the importance of such a field as it propagates as a non-diffractive beam. Instead of the Fresnel propagation a lens is included to disregard a quadratic multiplicative phase. The physical situation is depicted in figure 3.4.

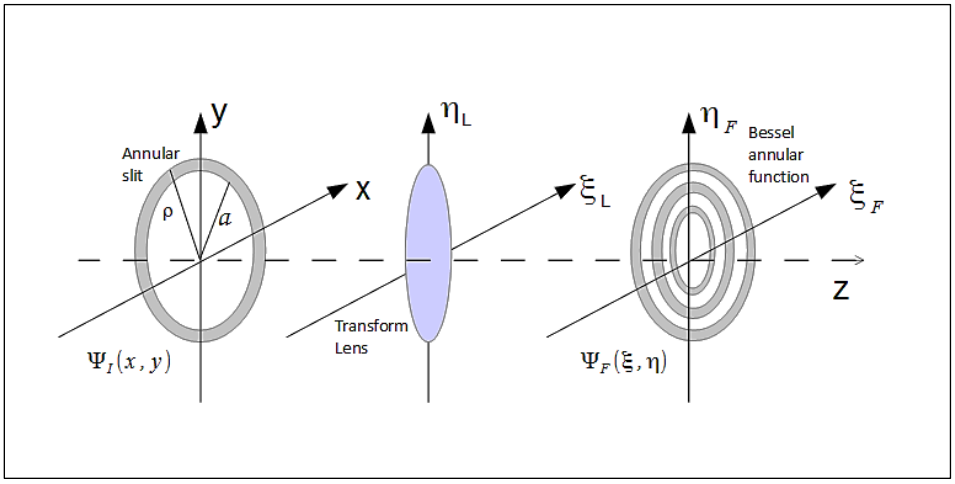

Figure 3.4. Experimental setup to generate an amplitude distribution of a Bessel function.

The annular function in the object plane is written as

$$\Psi(\rho) = \delta(\rho - a), \tag{3.29}$$

where δ is the Dirac delta function.

Using the lens as a Fourier transforming device, and using equation (3.23) the propagation at the back focal plane of the lens can be written as [29],

$$\Psi(r) = 2\pi \frac{e^{i\frac{2\pi}{\lambda}f}}{i\lambda f} \int_0^\infty \delta(\rho - a)\, \mathrm{J}_0\left(\frac{2\pi r\rho}{\lambda f}\right) \rho d\rho. \tag{3.30}$$

Using well known properties of the Dirac delta functions allow calculating the integral in equation (3.30) as

$$\Psi(r) = 2\pi \frac{e^{i\frac{2\pi}{\lambda}f}}{i\lambda f} \mathrm{J}_0\left(\frac{2\pi r a}{\lambda f}\right). \tag{3.31}$$

In chapter 4 it is shown in detail that the Bessel function given in equation (3.31) represents a non-diffractive beam; for this reason, instead of plotting the intensity distribution at the plane of observation as we have commonly done in the previous examples, we plot in figure 3.5 the normalized amplitude of this distribution.

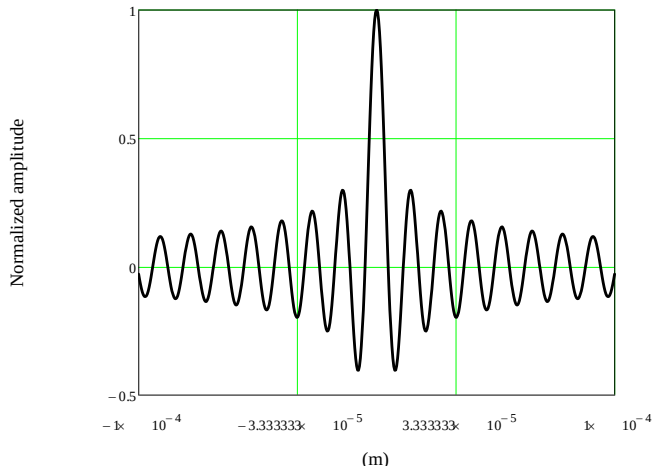

Figure 3.5. Normalized amplitude of the Bessel field at the plane of observation. $f = 10 \times 10^{-2}$ m, $a = 5 \times 10^{-3}$ m, $\lambda = 638 \times 10^{-9}$ m.

Chapter 4

Analytical methods for finding solutions leading to non-diffractive waves.

In this chapter we introduce analytical methods for solving the wave equation in free space. It will be seen that some of these methods will lead to non-diffractive waves and also to diffractive waves. Additionally some of these solutions will consist of optical pulses.

4.1 Solutions to the homogeneous wave equation in free space.

The wave equation in free space reads,

$$\left(\frac{\partial^2\psi(x,y,z;t)}{\partial x^2}+\frac{\partial^2\psi(x,y,z;t)}{\partial y^2}+\frac{\partial^2\psi(x,y,z;t)}{\partial z^2}-\frac{1}{c^2}\frac{\partial^2\psi(x,y,z;t)}{\partial t^2}\right)=0. \tag{4.1}$$

One of the methods suggested consists in writing the transversal part of the wave equation (4.1) in cylindrical coordinates (ρ,ϕ,z,t) to attain separated the z and t dependence [31,32]. The method is as follows.

Before solving equation (4.1) it is convenient to write it in axially symmetric cylindrical coordinates as,

$$\left(\frac{\partial^2}{\partial\rho^2}+\frac{1}{\rho}\frac{\partial}{\partial\rho}+\frac{\partial^2}{\partial z^2}-\frac{1}{c^2}\frac{\partial^2}{\partial t^2}\right)\psi(\rho,z;t)=0. \tag{4.2}$$

Now, to solve equation (4.1) we will proceed as follows.

First, we take again equation (4.2) and propose a solution given by,

$$\psi(x,y,z;t)=\psi_A(x,y)e^{i(k_z z-\omega t)}\,. \tag{4.3}$$

We now propose a Fourier method to solve equation (4.3). For this, we write $\psi_A(x,y)$ as a function of its inverse Fourier transform as,

$$\psi_A(x,y)=\iint_{-\infty}^{+\infty}\tilde{\psi}_A(u,v)e^{i2\pi(ux+vy)}dudv, \tag{4.4}$$

where (u,v) represent the corresponding Fourier coordinate to (x,y).

To obtain the cylindrical solution we propose cylindrical coordinates parameters as follows. Let,

$$k_x = 2\pi u \ , \quad k_y = 2\pi v \ , \tag{4.5}$$

$$x = \rho\cos\phi \ , \quad y = \rho\sin\phi \ , \tag{4.6}$$

$$k_x = k_\rho\cos\Theta \ , \quad k_y = k_\rho\sin\Theta \ . \tag{4.7}$$

Equation (4.4) can be rewritten as,

$$\psi_A(\rho,\Theta) = \frac{1}{(2\pi)^2}\int_0^{2\pi}\int_{-\infty}^{+\infty}\tilde{\psi}_A\left(k_\rho,\Theta\right)e^{ik_\rho\rho\cos(\Theta-\phi)}k_\rho dk_\rho d\Theta \ . \tag{4.8}$$

Now in order to attain physical meaning we must restrict $\tilde{\psi}_A\left(k_\rho,\Theta\right)$ to be periodic on the variable Θ. Then, $\tilde{\psi}_A\left(k_\rho,\Theta\right)$ can be represented by a Fourier series as,

$$\tilde{\psi}_A\left(k_\rho,\Theta\right) = \sum_{n=-\infty}^{+\infty}A_n\left(k_\rho\right)e^{-in\Theta} \ . \tag{4.9}$$

In equation (4.4) $\tilde{\psi}_A\left(k_\rho,\Theta\right)$ has a period 2π. The coefficients A_n must depend on k_ρ in order to be consistent.

Equation (4.8) can now be written as,

$$\psi_A(\rho,\Theta) = \frac{1}{(2\pi)^2}\sum_{n=-\infty}^{+\infty}\int_{-\infty}^{+\infty}k_\rho A_n\left(k_\rho\right)dk_\rho\int_0^{2\pi}e^{ik_\rho\rho\cos(\Theta-\phi)}e^{-in\Theta}\,d\Theta \ . \tag{4.10}$$

Now changing $\Theta-\phi=\Theta'$ and considering that the function inside the integral over Θ is periodic, leads to,

$$\psi_A(\rho) = \frac{1}{2\pi}\sum_{n=-\infty}^{+\infty}(i)^n e^{-in\phi}\int_{-\infty}^{\infty}k_\rho A_n\left(k_\rho\right)J_n\left(k_\rho\rho\right)dk_\rho \ . \tag{4.11}$$

In equation (4.11) J_n represents the Bessel-Function of the first kind n-order.

We can see that the equation (4.3) changes its dependency $\psi(x,y,z;t)$ to $\psi(\rho,z;t)$ because $\psi_A(\rho)$ depends on ρ only.

By this assumption and substituting equation (4.11) into equation (4.3) with its $\psi(\rho,z;t)$ form, we obtain

$$\psi(\rho,z;t) = \frac{1}{2\pi}\sum_{n=-\infty}^{+\infty}(i)^n e^{-in\phi}\int_{-\infty}^{\infty}k_\rho A_n\left(k_\rho\right)J_n\left(k_\rho\rho\right)dk_\rho e^{i(k_z z-\omega t)} \ . \tag{4.12}$$

As is well-known the most general solution is obtained as a linear combination over k_z and ω as,

$$\psi(\rho,z;t)=\frac{1}{2\pi}\sum_{n=-\infty}^{+\infty}(i)^n e^{-in\phi}\iiint_{-\infty}^{\infty}k_\rho A_n(k_\rho)J_n(k_\rho\rho)e^{i(k_z z-\omega t)}\,dk_\rho dk_z d\omega. \quad (4.13)$$

For the particular case $n=0$, equation (4.13) reduces to,

$$\psi(\rho,z;t)=\frac{1}{2\pi}\int_{\omega=-\infty}^{\infty}\int_{k_z=-\infty}^{\infty}\int_{k_\rho=0}^{\infty}k_\rho A_0(k_\rho)J_0(k_\rho\rho)\,e^{i(k_z z-\omega t)}\,dk_\rho dk_z d\omega. \quad (4.14)$$

Equation (4.14) represents a general solution of the wave equation in free space; that indeed is a valid solution of equation (4.2) and is demonstrated as follows. Taking equation (4.14), we obtain the following equations,

$$\frac{\partial^2\psi(\rho,z;t)}{\partial\rho^2}=\frac{1}{2\pi}\int_0^{\infty}\iint_{-\infty}^{+\infty}-{k_\rho}^2[-\frac{1}{\rho}J_1(k_\rho\rho)+k_\rho J_0(k_\rho\rho)]e^{ik_z z}e^{-i\omega t}A(k_\rho)dk_\rho dk_z d\omega, \quad (4.15)$$

$$\frac{1}{\rho}\frac{\partial\psi(\rho,z;t)}{\partial\rho}=\frac{1}{2\pi}\int_0^{\infty}\iint_{-\infty}^{+\infty}-\frac{{k_\rho}^2}{\rho}J_1(k_\rho\rho)\,e^{ik_z z}e^{-i\omega t}A(k_\rho)dk_\rho dk_z d\omega\,, \quad (4.16)$$

$$\frac{\partial^2\psi(\rho,z;t)}{\partial z^2}=\frac{1}{2\pi}\int_0^{\infty}-k_\rho{k_z}^2J_0(k_\rho\rho)e^{ik_z z}e^{-i\omega t}A(k_\rho)dk_\rho dk_z d\omega\,, \quad (4.17)$$

$$-\frac{1}{c^2}\frac{\partial^2\psi(\rho,z;t)}{\partial t^2}=-\frac{1}{2\pi c^2}\int_0^{\infty}\iint_{-\infty}^{+\infty}-\omega^2k_\rho J_0(k_\rho\rho)e^{ik_z z}e^{-i\omega t}A(k_\rho)dk_\rho dk_z d\omega\,, \quad (4.18)$$

to calculate the above equations we used the following recurrence equations,

$${J_m}'(x)=\frac{m}{x}J_m(x)-J_{m+1}(x), \quad (4.19)$$

$$J_{m+1}(x)=\frac{2m}{x}J_m(x)-J_{m-1}(x). \quad (4.20)$$

By adding equations (4.15) up to (4.18) we obtain,

$$-\left[{k_\rho}^2+{k_z}^2-\frac{\omega^2}{c^2}\right]\psi(\rho,z;t)=0 \quad (4.21)$$

Thus we have demonstrated that the solution satisfies the differential wave equation provided that,

$${k_z}^2=\frac{\omega^2}{c^2}-{k_\rho}^2\,. \quad (4.22)$$

For calculations at far fields, it is possible to neglect the contribution of evanescent waves by assuming,

$$k_z > 0 \ , \sqrt{\frac{\omega^2}{c^2} - {k_\rho}^2} > 0 \, . \tag{4.23}$$

Then the general solution to equation (4.13) for the case $n = 0$, can be written as,

$$\psi(\rho, z; t) = \int_0^{\frac{\omega}{c}} \iint_{-\infty}^{+\infty} k_\rho J_0(k_\rho \rho)\, e^{i\left(\sqrt{\frac{\omega^2}{c^2} - {k_\rho}^2}\right) z} e^{-i\omega t} A_0(k_\rho, \omega) dk_\rho d\omega. \tag{4.24}$$

Finally it is important to remark that $A_0(k_\rho, \omega)$ represents the spectrum of the object amplitude distribution in the $(x, y, z = 0)$ plane. As this variable performs an important role in the calculations we rename $A_0(k_\rho, \omega)$ as $S(k_\rho, \omega)$ to indicate as explicit as possible that this term is a spectral function that corresponds to the object amplitude distribution of the field. Then we rewrite (4.24) as

$$\psi(\rho, z; t) = \int_0^{\frac{\omega}{c}} \iint_{-\infty}^{+\infty} k_\rho J_0(k_\rho \rho)\, e^{i\left(\sqrt{\frac{\omega^2}{c^2} - {k_\rho}^2}\right) z} e^{-i\omega t} S(k_\rho, \omega) dk_\rho d\omega. \tag{4.25}$$

Equation (4.25) represents the main tool for obtaining solutions to the wave equation. In the following chapters we describe some methods to obtain different solutions to the wave equation in the free space. As indicated above, some of the solutions will represent non-diffractive waves or pulses and others will represent diffractive waves.

Chapter 5

Spectral functions to generate solutions to the wave equation.

In the last chapter we introduced the spectral function $S(k_\rho, \omega)$. In this chapter we explicitly show that this spectral function represents the key for obtaining different solutions to the wave equation in free space. In what follows we will describe some examples. Several of these examples will represent diffractive waves and others not, as it will show.

5.1 Gaussian beam

As a first case we will consider a spectral function localized at ω_0 modulated by Gaussian amplitude as

$$S(k_\rho, \omega) = e^{-a^2 {k_\rho}^2} \delta(\omega - \omega_0)\,. \tag{5.1}$$

We will show that this spectral function leads to the typical paraxial Gaussian beam.

By substituting equation (5.1) into (4.25) we obtain,

$$\psi(\rho, z; t) = \int_0^{\frac{\omega}{c}} \int_{-\infty}^{\infty} e^{-a^2 {k_\rho}^2} \delta(\omega - \omega_0) k_\rho J_0(k_\rho \rho)\, e^{i\left(\sqrt{\frac{\omega^2}{c^2} - {k_\rho}^2}\right) z} e^{-i\omega t} dk_\rho d\omega. \tag{5.2}$$

In equation (5.2) the integral over ω can readily be performed; however the integral over k_ρ cannot be calculated analytically. Then, we will find a paraxial approximation as follows.

We take a first order approximation of the square root as,

$$\sqrt{\frac{\omega^2}{c^2} - {k_\rho}^2} \approx \frac{\omega}{c} - \frac{{k_\rho}^2 c}{2\omega}\,. \tag{5.3}$$

Additionally we extend again the integral over k_ρ up to infinity to include evanescent waves. It seems that evanescent waves can be neglected, however extending the integral to infinity necessarily takes into account evanescent waves similarly as in the Fresnel diffraction integral. Then we obtain,

$$\psi(\rho,z;t) = e^{i\left(\frac{\omega_0 z}{c}-\omega_0 t\right)} \int_0^\infty e^{-\left(a^2+i\frac{cz}{2\omega_0}\right)k_\rho{}^2} J_0\left(k_\rho\rho\right)k_\rho dk_\rho \,. \tag{5.4}$$

There is not a straightforward way to calculate the integral in (5.4). Fortunately we can calculate the integral in an indirect way as follows. First, we consider the following inverse Fourier transform,

$$\mathcal{F}^{-1}\left\{e^{-a^2\left(u^2+v^2\right)}\right\} = \int_{-\infty}^{+\infty}\int_{-\infty}^{+\infty} e^{-a^2\left(u^2+v^2\right)} e^{i2\pi(ux+vy)} du\, dv. \tag{5.5}$$

With the Fourier properties listed in chapter 2 we obtain,

$$\mathcal{F}^{-1}\left\{e^{-a^2\left(u^2+v^2\right)}\right\} = \frac{\pi}{a^2} e^{-\pi^2\left(\frac{x^2+y^2}{a^2}\right)} \,. \tag{5.6}$$

Now, making the following variable changes in equations (5.5) and (5.6),

$$k_x = 2\pi u \;\;, k_y = 2\pi v \,, \tag{5.7}$$

$$x = \rho\cos\phi \,, \;\; y = \rho\sin\phi \,, \tag{5.8}$$

$$k_x = K\cos\Theta \,, \; k_y = K\sin\Theta \,, \tag{5.9}$$

substituting (5.7 - 5.9) into (5.5) leads to,

$$\int_0^\infty\int_0^{2\pi} \frac{1}{4\pi^2}\cdot e^{-a^2\frac{K^2}{4\pi^2}} e^{-iK\rho\cos(\Theta-\phi)} K dK d\Theta = \frac{\pi}{a^2} e^{-\pi^2\left(\frac{\rho^2}{a^2}\right)}, \tag{5.10}$$

which can be rewritten as,

$$\int_0^\infty K e^{-a^2\frac{K^2}{4\pi^2}} J_0(K\rho) dK = \frac{4\pi^2}{2a^2} e^{-\pi^2\left(\frac{\rho^2}{a^2}\right)} \,. \tag{5.11}$$

Finally it will be useful to define $a'^2 = \frac{a^2}{4\pi^2}$. Then the integral (5.11) leads,

$$\int_0^\infty K e^{-a'^2K^2} J_0(K\rho) dK = \frac{1}{2a'^2} e^{-\left(\frac{\rho^2}{4a'^2}\right)} \,. \tag{5.12}$$

Equation (5.12) can now be used to evaluate (5.4) by now defining $a'^2 = a^2 + i\frac{cz}{2\omega_0}$.

Then equation (5.4) has now been solved with the result,

$$\psi(\rho,z;t) = \frac{1}{2\left(a^2+i\frac{z}{2k_0}\right)} e^{-\left[\frac{\rho^2}{4\left(a^2+i\frac{z}{2k_0}\right)}\right]} e^{ik_0(z-ct)} \,, \tag{5.13}$$

where, for brevity we have introduced the wave number,

$$k_0 = \frac{\omega_0}{c}. \tag{5.14}$$

As anticipated, equation (5.13) represents the typical equation of the propagation of a Gaussian beam from its waist plane up to distance z as obtained with the Fresnel diffraction integral. Figure 5.1 shows how this Gaussian beam propagates while it travels along z.

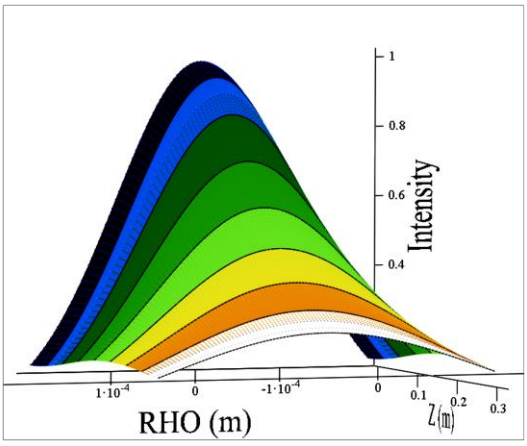

Figure 5.1 . a) Intensity of a Gaussian beam obtained with the spectral generating function (5.1) at different distances (z axis) , $c = 3 \times 10^8$ m/s, $\omega_0 = 3 \times 10^{15}$ s^{-1}, $a = 1 \times 10^{-4}\, m$.

The above result demonstrates that the spectral distribution proposed in equation (5.1) in combination with equation (4.25), in a paraxial approximation, is equivalent to the well-known solution of the propagation of a typical Gaussian beam.

5.2 Bessel beams

As a second case we will consider the following spectral distribution,

$$S(k_\rho, \omega) = \frac{\delta\left(k_\rho - \frac{\omega}{c}\sin\theta\right)}{k_\rho}\delta(\omega - \omega_0). \tag{5.15}$$

We will show that this spectral distribution yields the Bessel function of the first kind zero-order obtained in 1987 [7,16], which historically was reported as the first non-diffractive wave.

Substituting equation (5.15) into the general wave solution given by (4.25) we obtain the following expression,

$$\psi(\rho, z; t) = \int_0^\infty \int_{-\infty}^\infty \frac{\delta\left(k_\rho - \frac{\omega}{c}\sin\theta\right)}{k_\rho}\delta(\omega - \omega_0)\, k_\rho J_0\left(k_\rho \rho\right) e^{i\left(\sqrt{\frac{\omega^2}{c^2} - {k_\rho}^2}\right)z} e^{-i\omega t} dk_\rho d\omega \text{ , } \tag{5.16}$$

which can be readily evaluated as,

$$\psi(\rho, z; t) = e^{i\left(\sqrt{\frac{{\omega_0}^2}{c^2} - \left(\frac{\omega_0}{c}\sin\theta\right)^2}\right)z} e^{-i\omega_0 t} J_0\left(\frac{\omega_0}{c}\sin\theta\, \rho\right); \tag{5.17}$$

reducing terms we obtain,

$$\psi(\rho, z; t) = J_0\left(\frac{\omega_0}{c}\sin\theta\, \rho\right) e^{i\frac{\omega_0}{c}\cos\theta\left(z - \frac{ct}{\cos\theta}\right)}. \tag{5.18}$$

This beam exhibits velocity $v = \frac{c}{\cos\theta}$, and a transverse distribution represented by a Bessel function $J_0\left(\frac{\omega_0}{c}\sin\theta\, \rho\right)$.

It can be noticed that the amplitude of the wave given in equation (5.18) is independent of the distance of propagation z, thus representing a non-diffractive wave. Its property can be compared with the Gaussian beam that diffracts under propagation as illustrated in the plots in figure 5.2.

As indicated, the Bessel beam is non-diffractive. However this beam has infinite energy so it has to be truncated to be physically realizable. The consequences of this truncation are illustrated in the plots in figure 5.3.

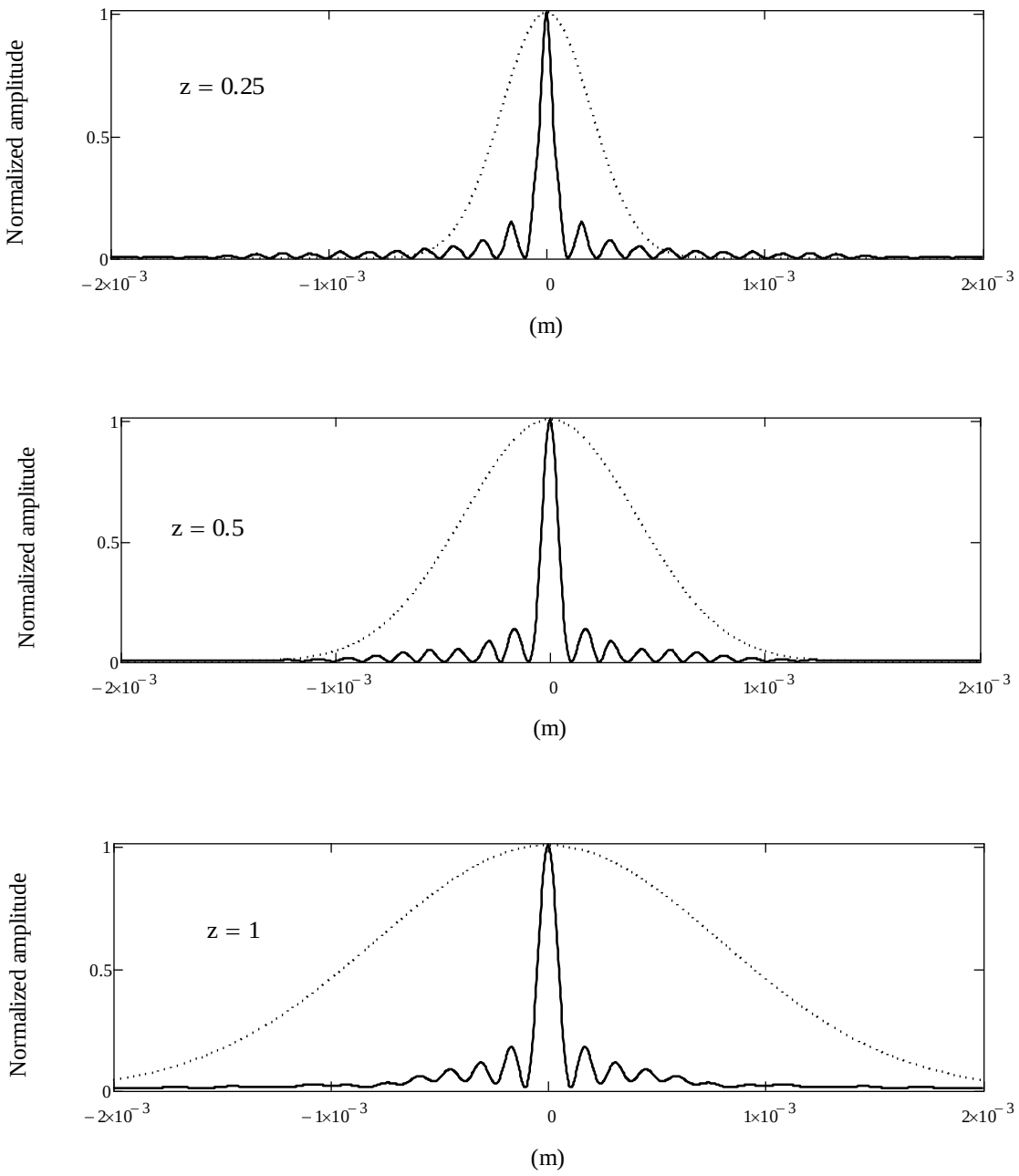

Figure 5.2. Comparative propagation intensity plots of a non-diffractive Bessel zero beam vs. Gaussian beam for different distances of propagation. The values of z are 0.25 m, 0.5 m and 1 m, $= 0.5 \times 10^{-6}$ m , $a = 24050\ \mathrm{m}^{-1}$; this value of a gives a central ring with a diameter of approximately 0.2 mm . The Bessel function was truncated to 15 rings.

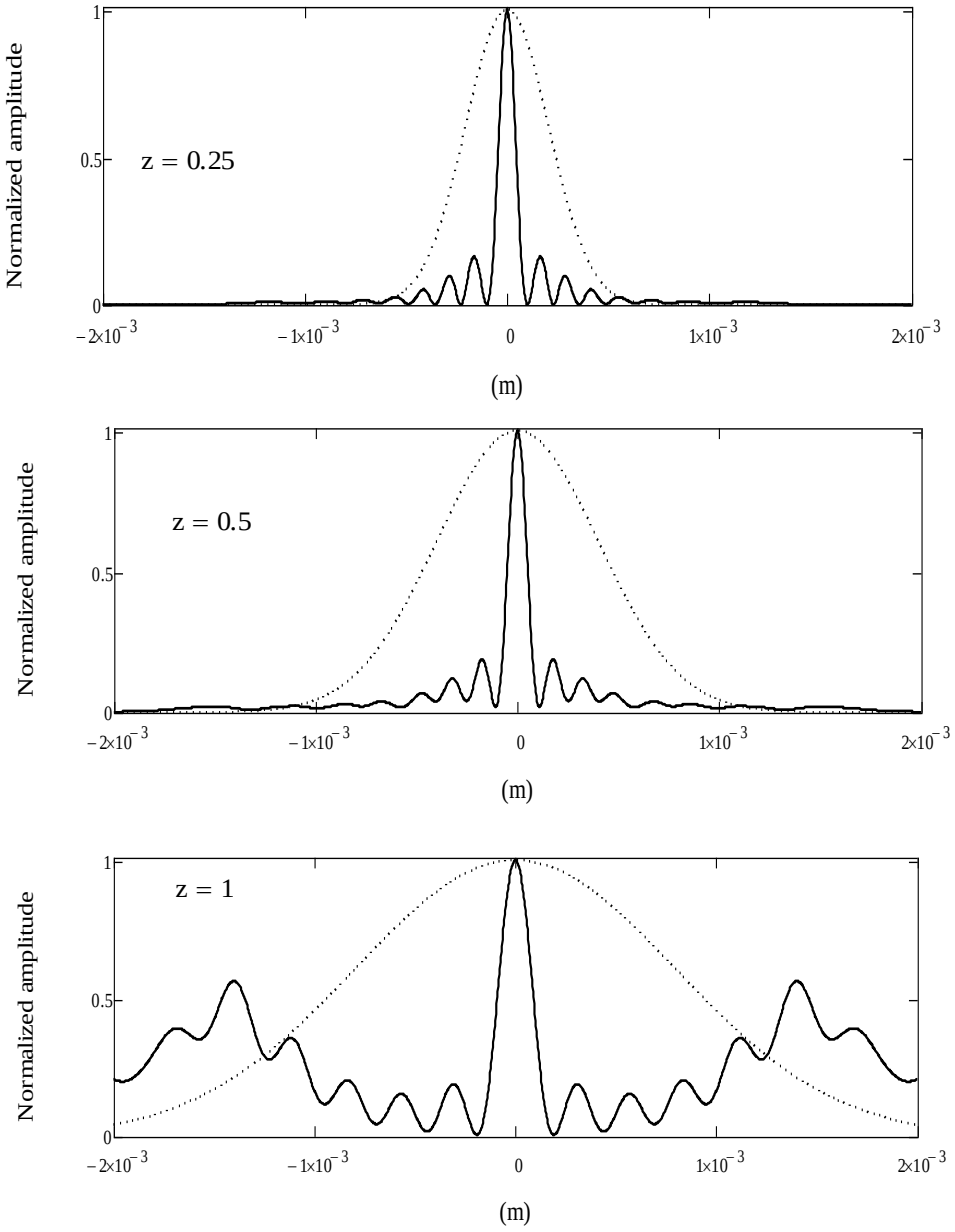

Figure 5.3. Comparative propagation intensity plots of a non-diffractive Bessel zero beam vs. Gaussian beam for different distances of propagation. The values of z are 0.25 m, 0.5 m and 1 m, $= 0.5 \times 10^{-6}$ m , $a = 24050\ \mathrm{m}^{-1}$; this value of a gives a central ring with a diameter of approximately 0.2 mm . The Bessel function was truncated to 8 rings.

As it can be seen from the above plots, the inherent necessity of truncating the Bessel beam inevitably reduces the non-diffractive depth of the beam, limiting its applicability.

An alternate way to visualize the non-truncated beam given by equation (5.18), is by means of a 3D plot while it evolves from $z = 0\ \mathrm{m}$, to $z = 1\ \mathrm{m}$ as illustrated in the following graphs in figure 5.4.

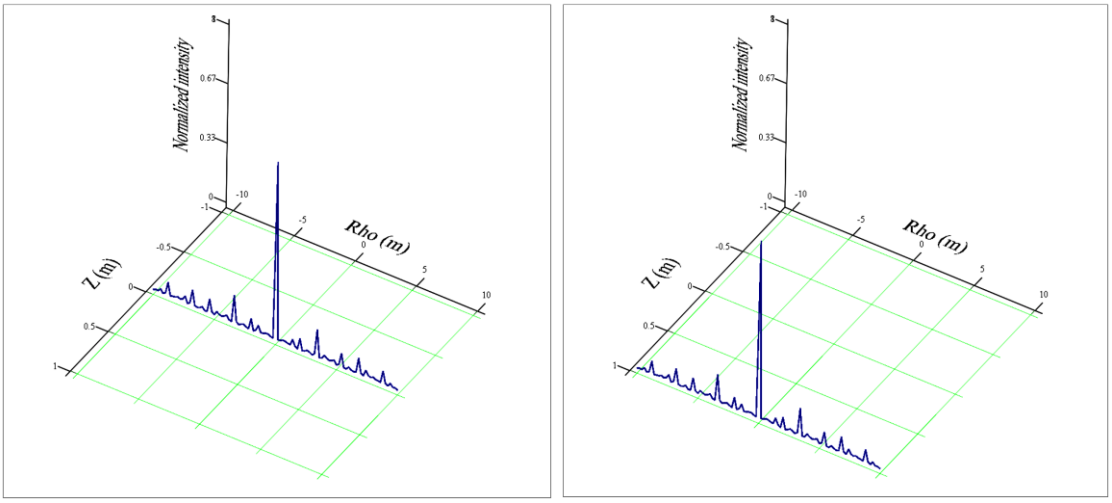

Figure 5.4. 3D plots of the propagation of a Bessel beam of the first kind zero- order as given by equation (5.18). The diameter size of the central ring was chosen arbitrarily.

5.3 Gaussian pulse

In this subsection we will consider the case,

$$S(k_\rho, \omega) = e^{-a^2 {k_\rho}^2} e^{-b^2(\omega-\omega_0)^2}. \tag{5.19}$$

In the paraxial region

$$\psi(\rho, z; t) = \int_0^\infty \int_{-\infty}^\infty e^{-a^2 {k_\rho}^2} e^{-b^2(\omega-\omega_0)^2}\, k_\rho J_0(k_\rho \rho)\, e^{i\left(\frac{\omega}{c} - \frac{{k_\rho}^2 c}{2\omega}\right)z} e^{-i\omega t} dk_\rho d\omega\,. \tag{5.20}$$

If we consider that the Gaussian has its maximum at ω_0 , then the contribution to the integral for this Gaussian comes from the ω_0 and the term $\frac{{k_\rho}^2 c}{2\omega}$. Under this condition it is possible to approximate,

$$\frac{{k_\rho}^2 c}{2\omega} \approx \frac{{k_\rho}^2 c}{2\omega_0} \quad . \tag{5.21}$$

Then, equation (5.20) can be written as

$$\psi(\rho, z; t) = \int_0^\infty k_\rho e^{-a^2 {k_\rho}^2} e^{-i\frac{{k_\rho}^2 cz}{2\omega_0}} J_0\left(k_\rho \rho\right) dk_\rho \int_{-\infty}^{\infty} e^{-b^2(\omega-\omega_0)^2} e^{i\left(\frac{z}{c}-t\right)\omega} d\omega, \tag{5.22}$$

for brevity, we define the integral over the k_ρ parameter as,

$$I_{k_\rho} = \int_0^\infty k_\rho e^{-a^2 {k_\rho}^2} e^{-i\frac{{k_\rho}^2 cz}{2\omega_0}} J_0\left(k_\rho \rho\right) dk_\rho \quad , \tag{5.23}$$

and the integral over the ω parameter as,

$$I_\omega = \int_{-\infty}^{\infty} e^{-b^2(\omega-\omega_0)^2} e^{i\left(\frac{z}{c}-t\right)\omega} d\omega \quad . \tag{5.24}$$

The integral I_{k_ρ} can be evaluate by the equation (5.12) and its result is,

$$I_{k_\rho} = \frac{1}{2\left(a^2 + i\frac{z}{2k_0}\right)} e^{-\frac{\rho^2}{4\left(a^2 + i\frac{z}{2k_0}\right)}} \quad . \tag{5.25}$$

The I_ω integral can be also analytical evaluated by rearranging the terms as follows,

$$I_\omega = e^{-b^2 {\omega_0}^2} \int_{-\infty}^{\infty} e^{-b^2\left\{\left(\omega - \frac{1}{2b^2}\left[2b^2\omega_0 + i\left(\frac{z}{c}-t\right)\right]\right)^2 - \frac{1}{4b^4}\left[2b^2\omega_0 + i\left(\frac{z}{c}-t\right)\right]^2\right\}} d\omega \, . \tag{5.26}$$

By defining,

$$s^2 = \left\{\omega - \frac{1}{2b^2}\left[2b^2\omega_0 + i\left(\frac{z}{c} - t\right)\right]\right\} \quad , \tag{5.27}$$

the integral (5.26) can be rewritten as

$$I_\omega = e^{-b^2 {\omega_0}^2} \cdot e^{\frac{1}{4b^2}\left[2b^2\omega_0 + i\left(\frac{z}{c}-t\right)\right]^2} \int_{-\infty}^{\infty} e^{-b^2 s^2} \, ds \quad , \tag{5.28}$$

and the result is,

$$I_\omega = \frac{\sqrt{\pi}}{b} e^{-b^2 {\omega_0}^2} \cdot e^{\frac{1}{4b^2}\left[2b^2\omega_0 + i\left(\frac{z}{c}-t\right)\right]^2}, \tag{5.29}$$

which can be expressed as

$$I_\omega = \frac{\sqrt{\pi}}{b} \cdot e^{\left[i\omega_0\left(\frac{z}{c}-t\right) - \frac{1}{4b^2}\left(\frac{z}{c}-t\right)^2\right]} . \tag{5.30}$$

So the final solution to equation (5.22) is,

$$\psi(\rho, z; t) = \frac{\sqrt{\pi}}{2b\left(a^2 + i\frac{z}{2k_0}\right)} e^{-\frac{\rho^2}{4\left(a^2 + i\frac{z}{2k_0}\right)}} e^{-\frac{1}{4b^2c^2}(z-ct)^2} e^{ik_0(z-ct)} . \tag{5.31}$$

Equation (5.31) represents a Gaussian pulse that travels along the axis z. As it propagates its width becomes wider as depicted in the plot in figure 5.5.

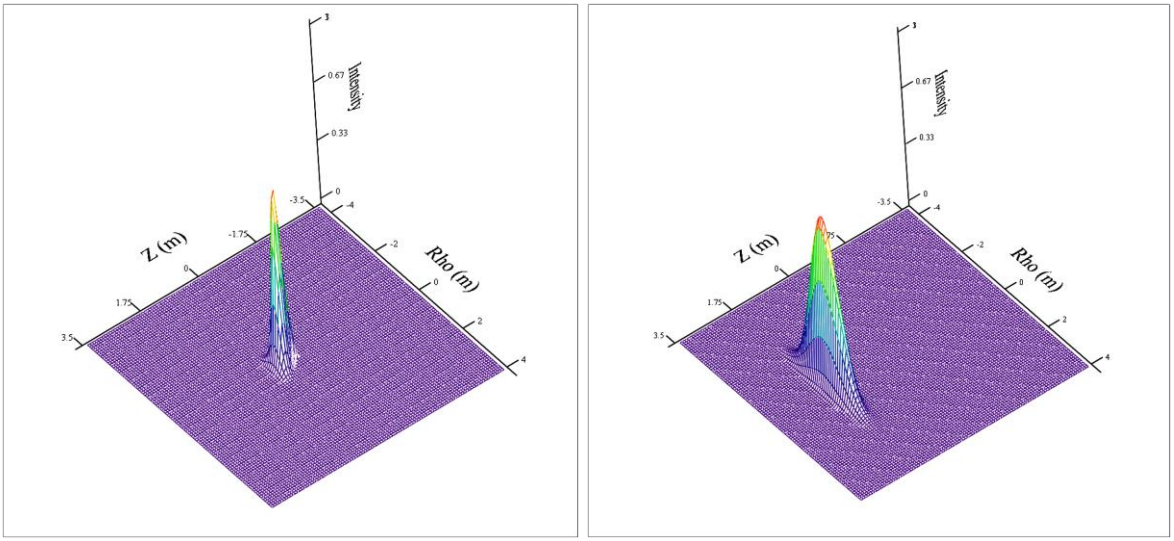

Figure 5.5. Gaussian pulse evolving in time $t = 0.15\ \mathrm{s}$ and $t = 0.55\ \mathrm{s}$ respectively; $a = 20 \times 10^{-3}\ \mathrm{m}$, $c = 3 \times 10^8\ \mathrm{m/s}$, $\omega_0 = 200 \times 10^8\ \mathrm{s}^{-1}$, $b = 40 \times 10^{-3}\ \mathrm{m}$.

5.4 Ordinary X- shaped pulses

Following the same procedure adopted in the previous section, let us construct ordinary X-shaped [2, 32] pulses by using spectral functions of the type

$$S(k_\rho, \omega) = S_1(k_\rho) S_2(\omega), \tag{5.32}$$

where $S_1(k_\rho)$ and $S_2(\omega)$ are,

$$S_1(k_\rho) = \frac{\delta\left(k_\rho - \frac{\omega}{c}\sin\theta\right)}{k_\rho} \quad , \qquad S_2(\omega) = \frac{a}{v}\,\mathrm{step}(\omega) e^{-\frac{a}{v}\omega} \quad , \tag{5.33}$$

where the step function, as usual, is defined as,

$$\mathrm{step}(\omega) = \begin{cases} 0 & -\infty < \omega < 0 \\ 1 & 0 \le \omega < \infty \end{cases}, \tag{5.34}$$

it will be useful the geometrical construction shown in figure 5.6,

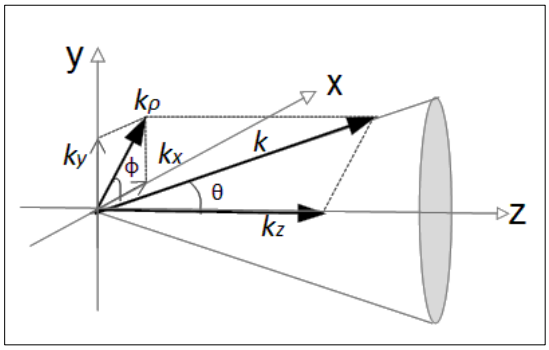

Figure 5.6. The wave vectors lay on the surface of a cone having the propagation axis z as its symmetry axis and angle equal to θ (also called “axicon angle”).

from this geometrical construction we have

$$k_\rho = k\sin\theta, \tag{5.35}$$

$$k_z = k\cos\theta, \tag{5.36}$$

and because by using equation (4.22) in chapter 4,

$$k_z{}^2 + k_\rho{}^2 = k^2 = \frac{\omega^2}{c^2}. \tag{5.37}$$

Substituting the above result and the spectral function (5.32) in equation (4.25) we obtain,

$$\psi(\rho,z;t)=\int_{-\infty}^{\infty}\int_{0}^{\infty}\delta\left(k_\rho-\frac{\omega}{c}\sin\theta\right)\frac{a}{v}\,\mathrm{step}(\omega)e^{-\frac{a}{v}\omega}J_0\left(k_\rho\rho\right)e^{i\left(\sqrt{\frac{\omega^2}{c^2}-{k_\rho}^2}\right)z}e^{-i\omega t}dk_\rho d\omega, \tag{5.38}$$

solving this integral leads

$$\psi(\rho,z;t)=\frac{a}{v}\int_{0}^{\infty}e^{-\frac{a}{v}\omega}J_0\left(\frac{\omega}{c}\sin\theta\,\rho\right)e^{i\left(\sqrt{\frac{\omega^2}{c^2}-\frac{\omega^2}{c^2}\sin\theta}\right)}e^{-i\omega t}d\omega\,, \tag{5.39}$$

which can be rewritten as

$$\psi(\rho,z;t)=\frac{a}{v}\int_{0}^{\infty}J_0\left(\frac{\omega}{c}\sin\theta\,\rho\right)e^{-\left[\frac{a}{v}-i\left(\frac{z}{c}\cos\theta-t\right)\right]\omega}d\omega, \tag{5.40}$$

using the equivalence $v=\frac{c}{\cos\theta}$, given in chapter 4, then we can regroup terms as

$$\psi(\rho,z;t)=\frac{a}{v}\int_{0}^{\infty}J_0\left(\frac{\omega}{c}\sin\theta\,\rho\right)e^{-\left[\frac{a}{v}-\frac{i}{v}(z-v\,t)\right]\omega}d\omega, \tag{5.41}$$

and making the following changes of variables,

$$\zeta=(z-v\,t)\,, \tag{5.42}$$

$$s=\frac{a-i\zeta}{v}, \tag{5.43}$$

$$\alpha=\frac{\sin\theta}{c}\rho\,, \tag{5.44}$$

the integral (5.41) can be rewritten as a Laplace transform as,

$$\psi(\rho,z;t)=\frac{a}{v}\int_{0}^{\infty}J_0(\alpha\omega)\,e^{-s\omega}d\omega\ . \tag{5.45}$$

This Laplace transform has the form

$$I=\int_{0}^{\infty}J_0(\alpha\omega)\,e^{-s\omega}d\omega=\int_{0}^{\infty}\left\{\frac{1}{2\pi}\int_{0}^{2\pi}e^{i\alpha\omega\sin\theta}e^{-in\theta}\,d\theta\right\}e^{-s\omega}\,d\omega, \tag{5.46}$$

then rearranging terms , equation (5.46) becomes

$$I=\frac{1}{2\pi}\int_{0}^{2\pi}e^{-in\theta}\,d\theta\int_{0}^{\infty}e^{-(s-i\alpha\sin\theta)}\,d\omega\,, \tag{5.47}$$

and evaluating the integral over the parameter ω, we can obtain the result

$$I=\frac{1}{2\pi}\int_{0}^{2\pi}\frac{e^{-in\theta}}{\left[s-\frac{\alpha}{2}\left(e^{i\theta}-e^{-i\theta}\right)\right]}d\theta\,. \tag{5.48}$$

Now, to perform the integral we use contour integration. Let,

$$z = e^{i\theta}\ , \tag{5.49}$$

$$dz = izd\theta. \tag{5.50}$$

Using this change in equation (5.48) leads to

$$I = \frac{1}{i2\pi}\oint_C \ \frac{z^{-n}}{\left[s-\frac{\alpha}{2}\left(z-\frac{1}{z}\right)\right]}\frac{dz}{z} \quad . \tag{5.51}$$

Now, we make the corresponding algebra to reach an expression of two factors in the denominator

$$I = -\frac{1}{i\pi}\oint_C \ \frac{z^{-n}}{[\alpha z^2-2sz-\alpha]}dz, \tag{5.52}$$

then we obtain the factors as follows

$$I = -\frac{1}{i\pi\alpha}\oint_C \ \frac{z^{-n}}{\left(z-\frac{s}{\alpha}\right)^2-\left(\frac{s^2}{\alpha^2}+1\right)}dz\ , \tag{5.53}$$

completing the square we obtain

$$I = -\frac{1}{i\pi\alpha}\oint_C \ \frac{z^{-n}}{\left\{\left(z-\frac{s}{\alpha}\right)-\left(\sqrt{\frac{s^2}{\alpha^2}+1}\right)\right\}\left\{\left(z-\frac{s}{\alpha}\right)+\left(\sqrt{\frac{s^2}{\alpha^2}+1}\right)\right\}}dz\ , \tag{5.54}$$

then:

$$I = -\frac{1}{i\pi\alpha}\oint_C \ \frac{z^{-n}}{\left\{z-\left[\frac{s}{\alpha}+\left(\frac{\sqrt{s^2+\alpha^2}}{\alpha}\right)\right]\right\}\left\{z-\left[\frac{s}{\alpha}-\left(\frac{\sqrt{s^2+\alpha^2}}{\alpha}\right)\right]\right\}}dz\ . \tag{5.55}$$

This complex integral has two poles at

$$P_1 = \left[\frac{s}{\alpha}+\left(\frac{\sqrt{s^2+\alpha^2}}{\alpha}\right)\right]\ , \qquad P_2 = \left[\frac{s}{\alpha}-\left(\frac{\sqrt{s^2+\alpha^2}}{\alpha}\right)\right]. \tag{5.56}$$

We suppose P_1 inside of the contour *C* then the integral (5.55) result

$$I_1 = \left(-\frac{2}{\alpha}\right)\frac{\left[\left(\frac{s+\sqrt{s^2+\alpha^2}}{\alpha}\right)\right]^{-n}}{\left\{\left[\frac{s}{\alpha}+\left(\frac{\sqrt{s^2+\alpha^2}}{\alpha}\right)\right]-\left[\frac{s}{\alpha}-\left(\frac{\sqrt{s^2+\alpha^2}}{\alpha}\right)\right]\right\}}\ , \tag{5.57}$$

finally we get

$$I_1 = -\frac{\alpha^n}{\left\{\sqrt{s^2+\alpha^2}\left(s+\sqrt{s^2+\alpha^2}\right)^n\right\}} \ . \tag{5.58}$$

We work with the above result to obtain an X-wave pulse, moreover, another case can be studied if P_2 resides inside of the contour *C*. In this case,

$$I_2 = \frac{\alpha^n}{\left\{\sqrt{s^2+\alpha^2}\left(s-\sqrt{s^2+\alpha^2}\right)^n\right\}} \ . \tag{5.59}$$

Once we have obtained the Laplace transform result, equation (5.45) is rewritten as

$$\psi(\rho, z; t) = \frac{a}{v}\frac{\alpha^n}{\sqrt{s^2+\alpha^2}\left[s+\sqrt{s^2+\alpha^2}\right]^n} \ . \tag{5.60}$$

Because we have $\alpha = \frac{\sin\theta}{c}\rho$, and $v = \frac{c}{\cos\theta}$, we can rewrite

$$\alpha^2 = \left(\frac{v^2}{c^2} - 1\right)\rho^2 \ , \tag{5.61}$$

then, for the particular case $n = 0$ the solution (5.60) becomes

$$\psi(\rho, \zeta) = \frac{a}{v}\frac{1}{\sqrt{\left(\frac{a-i\zeta}{v}\right)^2 + \frac{1}{v^2}\left(\frac{v^2}{c^2}-1\right)\rho^2}} \ . \tag{5.62}$$

Finally we have

$$\psi(\rho, \zeta) = \frac{a}{\sqrt{(a-i\zeta)^2 + \left(\frac{v^2}{c^2}-1\right)\rho^2}}, \tag{5.63}$$

which in terms of $(\rho, z - vt)$ is

$$\psi(\rho, z-vt) = \frac{a}{\sqrt{(a-i(z-vt))^2 + \left(\frac{v^2}{c^2}-1\right)\rho^2}} \ . \tag{5.64}$$

Equation (5.64) is the well-known ordinary X-wave pulse solution reported by several authors [9, 12], this X-wave does not spread while it travels along the z axes. Figure 5.7 depicts an X-wave pulse as it evolves in time.

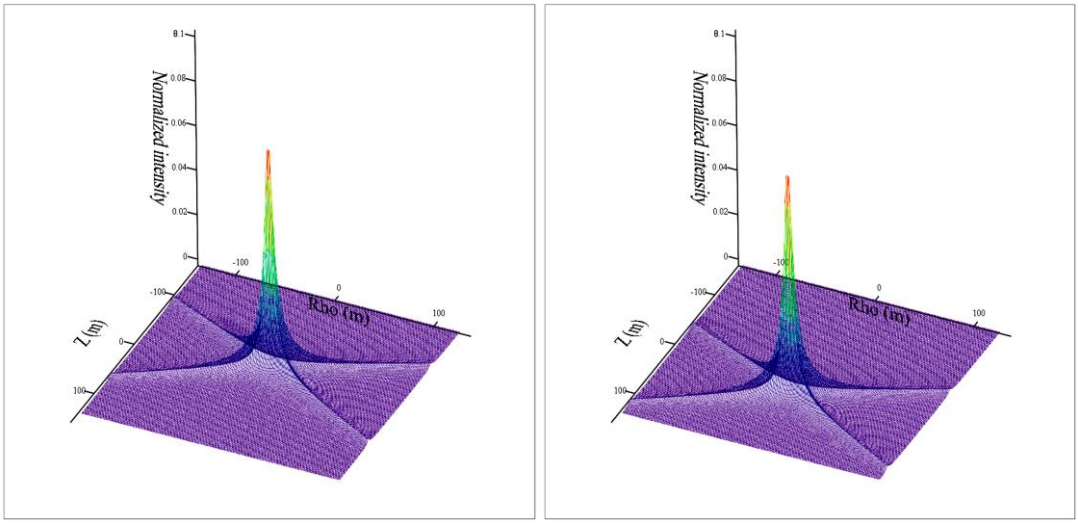

Figure 5.7. Propagation of an X-wave pulse for $c = 3 \times 10^8$ m/s, $v = 3.5 \times 10^8$ m/s, $a = 3$ m, $b = 40 \times 10^{-3}$ m, as it evolves for $t = 0$ s, $t = 15$ s, respectively.

It will be noticed that the velocity of propagation of the X-wave was selected with a value $v = 3.5 \times 10^8$ m/s which is $> c$. This type of wave is known as a tachyon [33]. It has additionally being shown experimentally its existence [27,34]. However these preliminary experiments have been performed with acoustic waves; it still remains the challenge to show experimental evidence of tachyons for electromagnetic waves.

X-wave pulses have infinite energy like the Bessel ideal beam described above. Thus, a truncated X-wave pulse is necessary to perform a realistic experiment. In this direction preliminary experimental evidence has been reported using acoustic waves [11,12]. In this report the truncated X-waves have shown to maintain their spatial shape for some depth in a similar way as the Bessel truncated beams.

Before finishing this section we present table 5.1 to summarize the different spectral distributions described and their corresponding amplitude distributions.

$S(k_\rho, \omega)$	$\psi(\rho, z; t)$	***Non-diffractive***
$e^{-a^2 {k_\rho}^2}\delta(\omega-\omega_0)$	$\frac{1}{2\left(a^2+i\frac{z}{2k_0}\right)} e^{-\left[\frac{\rho^2}{4\left(a^2+i\frac{z}{2k_0}\right)}\right]} e^{ik_0(z-ct)}$ ***(Gaussian Beam)***	
$\frac{\delta\left(k_\rho-\frac{\omega}{c}\sin\theta\right)}{k_\rho} \cdot \delta(\omega-\omega_0)$	$J_0\left(\frac{\omega_0}{c}\sin\theta\,\rho\right) e^{i\frac{\omega_0}{c}\cos\theta\left(z-\frac{ct}{\cos\theta}\right)}$ ***(Bessel Beam)***	✓
$e^{-a^2 {k_\rho}^2} e^{-b^2(\omega-\omega_0)^2}$	$\frac{\sqrt{\pi}}{2b\left(a^2+i\frac{z}{2k_0}\right)} e^{-\frac{\rho^2}{4\left(a^2+i\frac{z}{2k_0}\right)}} e^{-\frac{1}{4b^2c^2}(z-ct)^2} e^{ik_0(z-ct)}$ ***(Gaussian Pulse)***	
$\frac{\delta\left(k_\rho-\frac{\omega}{c}\sin\theta\right)}{k_\rho} \cdot \frac{a}{v}\text{step}(\omega) e^{-\frac{a}{v}\omega}$	$\frac{a}{\sqrt{(a-i(z-vt))^2+\left(\frac{v^2}{c^2}-1\right)\rho^2}}$ ***(X –wave Pulse)***	✓

Table 5.1. Spectral functions with their respect wave solution and their non-diffractive property.

5.5 Example of a Gaussian pulse obtained by another method.

In previous sections we had worked with the spectral function to generate solutions to the wave equation. In this section we will follow a different approach for obtaining such solutions. Some of the solutions that will be obtained have been implemented and suited by means of experimental observations.

In this technique we assume a solution to the wave equation (4.1) of the form,

$$\psi(x,y,z;t) = e^{ik(z+ct)}F\big(x,y,(z-ct)\big)\,. \tag{5.65}$$

For brevity, we define the parameter,

$$\tau = z_0 + i(z-ct), \tag{5.66}$$

To proceed further we calculate the first and second partial derivatives of $F(x,y,\tau)$,

$$\frac{\partial F}{\partial z} = i\frac{\partial F}{\partial \tau} \quad , \quad \frac{\partial^2 F(x,y,\tau)}{\partial z^2} = -\frac{\partial^2 F(x,y,\tau)}{\partial \tau^2}\,, \tag{5.67}$$

$$\frac{\partial F}{\partial t} = -ic\frac{\partial F}{\partial \tau} \quad , \quad \frac{\partial^2 F(x,y,\tau)}{\partial t^2} = -c^2\frac{\partial^2 F(x,y,\tau)}{\partial \tau^2}\,. \tag{5.68}$$

Which leads to,

$$\frac{\partial^2 \psi(x,y,z;t)}{\partial z^2} = e^{ik(z+ct)}\left\{-k^2F(x,y,\tau) + i2k\frac{i\partial F}{\partial \tau} - \frac{\partial^2 F}{\partial \tau^2}\right\}, \tag{5.69}$$

and,

$$\frac{\partial^2 \psi(x,y,z;t)}{\partial t^2} = e^{ik(z+ct)}\left\{-k^2c^2F(x,y,\tau) + (i2kc)(-ic)\frac{\partial F}{\partial \tau} - c^2\frac{\partial^2 F}{\partial \tau^2}\right\}. \tag{5.70}$$

Adding both terms (5.69) and (5.70) we obtain the expression

$$\frac{\partial^2 \psi(x,y,z;t)}{\partial z^2} - \frac{1}{c^2}\frac{\partial^2 \psi(x,y,z;t)}{\partial t^2} = e^{ik(z+ct)}\left(-4k\frac{\partial F(x,y,\tau)}{\partial \tau}\right), \tag{5.71}$$

substituting (5.71) in equation (4.1) , the wave equation becomes

$$\left(\frac{\partial^2 F(x,y,\tau)}{\partial x^2} + \frac{\partial^2 F(x,y,\tau)}{\partial y^2} = 4k\frac{\partial F(x,y,\tau)}{\partial \tau}\right), \tag{5.72}$$

which is a Schrödinger-kind equation.

To solve equation (5.72) we will follow a Fourier transforming technique.

The function $F(x,y,\tau)$ can be expressed as a Fourier transform as follows

$$F(x,y,\tau) = \iint_{-\infty}^{\infty} \tilde{F}(u,v,\tau) e^{i2\pi(ux+vy)} du dv \,, \tag{5.73}$$

similarly,

$$F(x) = \int_{-\infty}^{\infty} F(u) e^{i2\pi ux} du \;, \quad F(y) = \int_{-\infty}^{\infty} F(v) e^{i2\pi vy} dv \,, \tag{5.74}$$

$$\frac{dF(x)}{dx} = \frac{d}{dx}\left(\int_{-\infty}^{\infty} F(u) e^{i2\pi ux} du\right) = i2\pi u \int_{-\infty}^{\infty} F(u) e^{i2\pi ux} du \,, \tag{5.75}$$

then,

$$F''(x) = -4\pi^2 u^2 \tilde{F}(u) \;, F''(y) = -4\pi^2 v^2 \tilde{F}(v) \,, \tag{5.76}$$

substituting (5.76) in equation (5.72) we obtain

$$\pi^2(u^2+v^2)\tilde{F}(u,v,\tau) + k\frac{\partial \tilde{F}(u,v,\tau)}{\partial \tau} = 0 \,. \tag{5.77}$$

To solve (5.77), as usually, we propose,

$$\tilde{F}(u,v,\tau) = Ae^{\lambda\tau} \;. \tag{5.78}$$

Substituting equation (5.78) in equation (5.77) gives,

$$\pi^2(u^2+v^2) + k\lambda = 0 \,, \tag{5.79}$$

thus

$$\lambda = -\frac{\pi^2(u^2+v^2)}{k} \;. \tag{5.80}$$

Then equation (5.78) becomes

$$\tilde{F}(u,v,\tau) = Ae^{-\frac{\pi^2(u^2+v^2)}{k}\tau} \,, \tag{5.81}$$

substituting (5.81) into (5.73) leads

$$F(x,y,\tau) = A\iint_{-\infty}^{\infty} e^{-\frac{\pi^2(u^2+v^2)}{k}\tau} e^{i2\pi(ux+vy)} du dv = AI_1 I_2 \,, \tag{5.82}$$

where

$$I_1 = \sqrt{\frac{k}{\pi\tau}}\, e^{\frac{k}{\tau}x^2}\ , \tag{5.83}$$

and

$$I_2 = \sqrt{\frac{k}{\pi\tau}}\, e^{\frac{k}{\tau}y^2}\ , \tag{5.84}$$

finally

$$F(x,y,\tau) = \frac{1}{4\pi i\tau}\, e^{\frac{k}{\tau}(x^2+y^2)}\ , \tag{5.85}$$

substituting in equation (5.65)

$$\psi(x,y,z;t) = \frac{1}{4\pi i\tau}\, e^{ik(z+ct)} e^{\frac{k}{\tau}(x^2+y^2)}, \tag{5.86}$$

in terms of $z_0 + i(z-ct)$ we obtain,

$$\psi(\rho,z;t,\tau) = \frac{1}{4\pi i}\, \frac{e^{\frac{k}{[z_0+i(z-ct)]}(\rho^2)}}{[z_0+i(z-ct)]}\, e^{ik(z+ct)}\ . \tag{5.87}$$

Equation (5.87) is a modulated non-diffractive traveling Gaussian pulse. In particular, this pulse recovers its initial amplitude along a specified direction of propagation at very large distances from their initial location. If z_0 increases, its amplitude decreases.

A time sequence of the fundamental solution equation (5.87) is shown in figure 5.8.

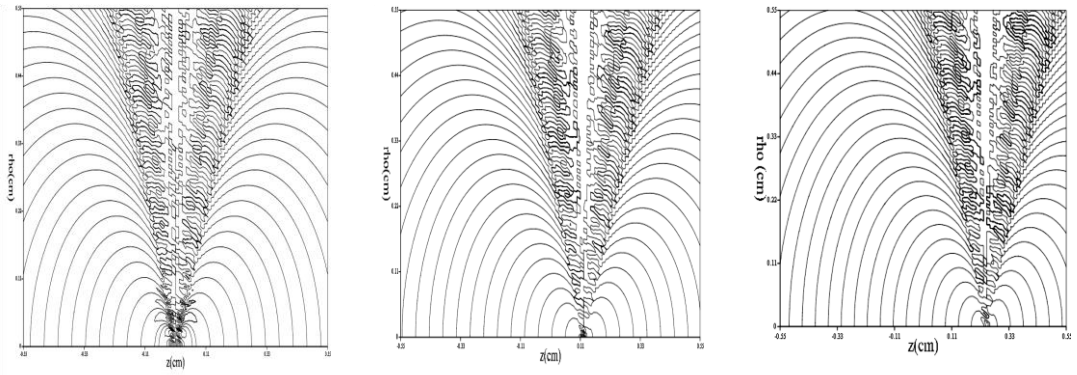

Figure 5.8 . Contours of the Gaussian pulse as it evolves with time; $t = 0\ s$, $t = 4\ s$, and $t = 8\ s$.

An intensity plot of this Gaussian pulse is shown in figure 5.9 to visualize that the pulse does not diffract while it is traveling along *z.*

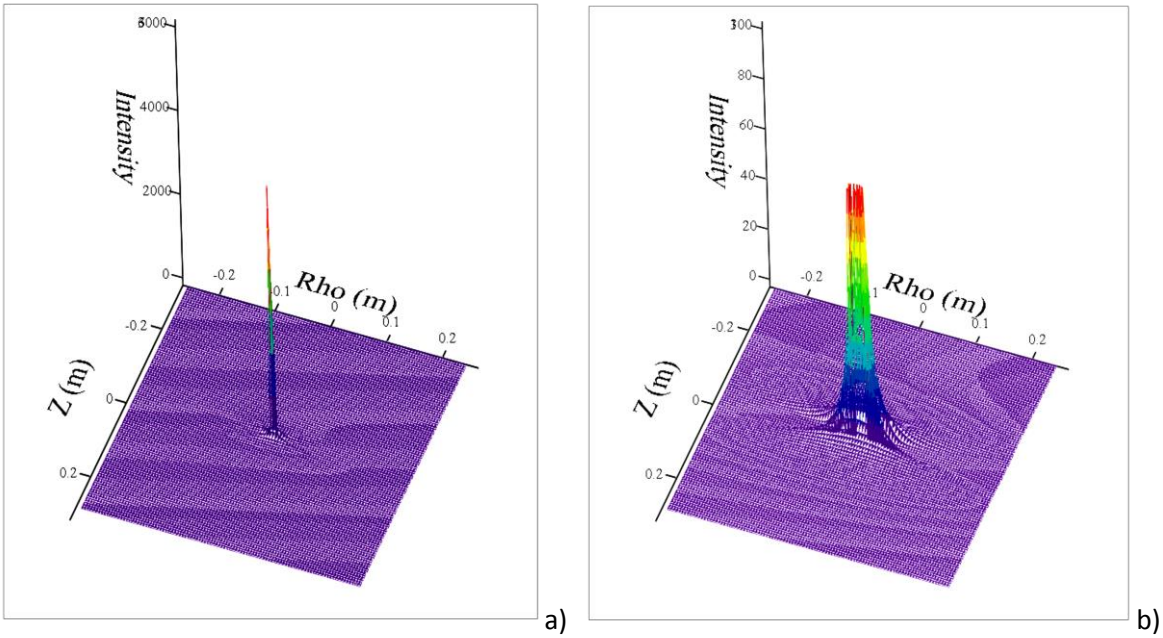

a) b)

Figure 5.9 This Gaussian pulse is traveling along z axis without spreading. a) This plot shows that it is very intense in a small region thus b) is a zoom of this pulse to see its constant width with more detail.

In summary, we demonstrated that the differential wave equation in free space can be solved by two different techniques. One of these techniques uses the spectral complex amplitude distribution located at the object plane; the other technique is a result of proposing different analytical forms working directly in the wave equation. A classification of the properties of the solutions obtained with the spectral function was summarized in a table 5.1 . It is clear that new solutions can be found by proposing different spectral functions.

Chapter 6

Non-diffractive Mathieu Beam

In this chapter we describe non-diffractive beams based on Mathieu functions. We show that these functions are exact solutions to the wave equation. The propagation of Mathieu beams can be calculated by using the Whittaker integral as described in this chapter.

6.1 Mathieu functions

For convenience we repeat here the wave equation in free space in Cartesian coordinates written as the Helmholtz equation as,

$$\left(\frac{\partial^2}{\partial x^2}+\frac{\partial^2}{\partial y^2}+\frac{\partial^2}{\partial z^2}+k^2\right)\psi(x,y,z)=0\ . \tag{6.1}$$

We now introduce elliptical cylindrical coordinates,

$$x = p\cosh\xi\cos\eta, \tag{6.2.1}$$

$$y = p\sinh\xi\sin\eta. \tag{6.2.2}$$

By substituting (6.2.1) and (6.2.2) into (6.1) the Helmholtz equation reads,

$$\left[\frac{1}{p^2(\cosh^2\xi-\cos^2\eta)}\left(\frac{\partial^2}{\partial\xi^2}+\frac{\partial^2}{\partial\eta^2}\right)+\frac{\partial^2}{\partial z^2}+k^2\right]\psi(\xi,\eta,z;t)=0\,. \tag{6.3}$$

To solve equation (6.3) the solution is typically written as

$$\psi(\xi,\eta,z)=F(\xi)G(\eta)\mathrm{Z}(z)\ . \tag{6.4}$$

Substituting (6.4) into (6.3) we obtain the following equation

$$\frac{1}{p^2(\cosh^2\xi-\cos^2\eta)}\left(\frac{1}{F}\frac{\partial^2F}{\partial\xi^2}+\frac{1}{G}\frac{\partial^2G}{\partial\eta^2}\right)+\frac{1}{\mathrm{Z}}\frac{\partial^2\mathrm{Z}}{\partial z^2}+k^2=0\ . \tag{6.5}$$

Equation (6.5) can be separated in the following three equations,

$$\frac{\partial^2\mathrm{Z(z)}}{\partial z^2}+(k^2-m^2)\mathrm{Z(z)}=0\,, \tag{6.6.1}$$

$$\frac{d^2G(\eta)}{d\eta^2}+(a-2q\cos2\eta)G(\eta)=0\,, \tag{6.6.2}$$

$$\frac{d^2F(\xi)}{d\xi^2}-(a-2q\cosh2\xi)F(\xi)=0\,. \tag{6.6.3}$$

In equations (6.6.1) to (6.6.3) m and a are constants obtained from the method of separation variables. q and k_z for brevity are defined as

$$q = \frac{m^2 p^2}{4} \ , \tag{6.7.1}$$

$$k_z = \sqrt{k^2 - m^2} \ . \tag{6.7.2}$$

The longitudinal differential equation has the solution

$$\mathrm{Z(z)} = e^{\pm i k_z z} \ . \tag{6.8}$$

Equation (6.6.2) and (6.6.3) are known as the Mathieu´s ordinary and modified differential equations respectively [35].

Before proceeding further, it is important to remark that the modified Mathieu differential equation can be written as an ordinary Mathieu differential equation by writing $\xi \to -i\xi$. Thus it is only necessary to solve the ordinary Mathieu differential equation.

The ordinary Mathieu differential equation is solved by proposing four possible series as follows,

$$ce_{2n}(q,\eta) = \sum_{n=0}^{\infty} A_{2n} \cos(2n\eta), \tag{6.9.1}$$

$$ce_{2n+1}(q,\eta) = \sum_{n=0}^{\infty} A_{2n+1} \cos\big((2n+1)\eta\big), \tag{6.9.2}$$

$$se_{2n+2}(q,\eta) = \sum_{n=0}^{\infty} B_{2n+2} \sin\big((2n+2)\eta\big), \tag{6.9.3}$$

$$se_{2n+1}(q,\eta) = \sum_{n=0}^{\infty} B_{2n+1} \sin\big((2n+1)\eta\big). \tag{6.9.4}$$

As it can be seen the four possibilities consist in cosine series (even or odd) and sine series (even or odd). ce stands for cosine elliptic and se for sine elliptic.

In the following subsection we will find the coefficients of the above series.

6.2 Solution to the ordinary Mathieu differential equation. Characteristics values.

We will begin solving equation (6.9.1). Substituting (6.9.1) into (6.6.2) gives the following recursive relations,

$$\sum_{n=0}^{\infty}[a-(2n)^2]\cdot A_{2n}\cos(2n\eta)-q\sum_{n=0}^{\infty}A_{2n}\cos\big((2n+2)\eta\big)$$

$$-q\sum_{n=0}^{\infty}A_{2n}\cos\big((2n-2)\eta\big)\,. \tag{6.10}$$

Using equation (6.10), we obtain

$$\text{for } n=0, \text{ then} \qquad aA_0-qA_2=0, \tag{6.11.1}$$

$$\text{for } n=1, \text{ then} \qquad -2qA_0+[a-4]A_2-qA_4=0, \tag{6.11.2}$$

$$\text{for } n=2, \text{ then} \qquad -qA_2+[a-16]A_4-qA_6=0. \tag{6.11.3}$$

The general term is given by

$$\text{for } n\geq 2, \text{ then} \qquad [a-4n^2]A_{2n}-q(A_{2n-2}+A_{2n+2})=0. \tag{6.11.4}$$

The above relations can be written in matrix form as,

$$\begin{pmatrix} a & -q & 0 & 0 & 0 \\ -2q & a-4 & -q & 0 & 0 \\ 0 & 0 & -q & a-36 & -q \\ \dots & \dots & \dots & \dots & \dots \\ \dots & \dots & \dots & \dots & \dots \end{pmatrix}\begin{pmatrix} A_0 \\ A_2 \\ A_3 \\ A_4 \\ \dots \end{pmatrix}=\begin{pmatrix} 0 \\ 0 \\ 0 \\ 0 \\ \dots \end{pmatrix}. \tag{6.12}$$

In order to obtain non trivial solutions the determinant of the left matrix must be zero. However the matrix has an infinite number of terms and for its calculation it has necessarily to be truncated. However even truncated the matrix involves difficulties. Thus, we will use a recurrence method as follows.

As a first step we consider the sub-determinant that consists of the first four elements,

$$\begin{vmatrix} a & -q \\ -2q & (a-4) \end{vmatrix}=a(a-4)-2q^2=0\,. \tag{6.13}$$

Equation (6.13) shows that a is a function of q. The value obtained for a is referred as the characteristic value and it has to be iterated to obtain the best estimation. From (6.13) we obtain two possible values for a,

$$a_1 = 2 + \frac{q^2}{2}, \tag{6.14.1}$$

$$a_2 = -\frac{q^2}{2}. \tag{6.14.2}$$

As it can be seen we have obtained two characteristic values a_1 and a_2 by taking a matrix of two by two elements. As it can be seen the matrix has an infinite number of elements, thus, there will be an infinite number of characteristic values. It is customary to order all the characteristic values from lower to higher and denoted them as $a_1, a_2, a_3, \ldots$ Accordingly the solution that corresponds to the characteristic value a_n is known as the Mathieu function of order – n.

As an example we take (6.14.2) to calculate the Mathieu function of order zero by taking (6.14.2) as the minimum characteristic value, then, accordingly we re-define

$$a_0 = -\frac{q^2}{2}. \tag{6.15}$$

As indicated this is not the final value for a_0, an iteration is necessary to find a better estimation. We will use the following procedure.

We propose

$$a_0 = -\frac{q^2}{2} + \Delta a, \tag{6.16}$$

where Δa is a small value that will be calculated.

Additionally we define scaling terms as follows,

$$v_0 A_0 = A_2, \tag{6.17.1}$$

$$v_2 A_2 = v_2 v_0 A_0 = A_4, \tag{6.17.2}$$

$$v_4 A_4 = v_4 v_2 v_0 A_0 = A_6. \tag{6.17.3}$$

In general,

$$A_{n+2} = v_n A_n. \tag{6.17.4}$$

We now use (6.11.1) to (6.11.3) as follows,

$$(a_0 + \Delta a)A_0 - qv_0A_0 = 0, \tag{6.18.1}$$

$$-2qA_0 + (a_0 + \Delta a - 4)v_0A_0 - qv_2v_0A_0 = 0, \tag{6.18.2}$$

$$-qA_2 + (a_0 + \Delta a - 16)v_2A_2 - qv_4v_2A_2 = 0. \tag{6.18.3}$$

Equations (6.18.1) to (6.18.3) give

$$(a_0 + \Delta a) = qv_0 \ , \tag{6.19.1}$$

$$v_0 = \frac{2q}{a_0+\Delta a-4-qv_2}, \tag{6.19.2}$$

$$v_2 = \frac{q}{a_0+\Delta a-16-qv_4}. \tag{6.19.3}$$

Combining (6.19.1) to (6.19.3) gives,

$$a_0 + \Delta a = \frac{2q^2}{a_0+\Delta a-4-\frac{q^2}{a_0+\Delta a-16-qv_4}}. \tag{6.19.4}$$

Using a first order approximation in (16.9.4) gives

$$\Delta a = \frac{7q^4}{128} + \frac{q^6}{64^2}\,. \tag{6. 19.5}$$

Using (6.19.5) gives

$$a = -\frac{q^2}{2} + \frac{7q^4}{128} + \frac{q^6}{64^2}. \tag{6.19.6}$$

The method is iterated as many times as desired. Each iteration improves the accuracy.

Now we are going to obtain the corresponding Mathieu function.

$$ce_0(q,\eta) = A_0 + A_2\cos(2\eta) + A_4\cos(4\eta) + \cdots, \tag{6.20}$$

$$ce_0(q,\eta) = A_0(1 + v_0\cos(2\eta) + v_2v_0\cos(4\eta) + \cdots). \tag{6.20.1}$$

In (6.20.1) the values of v_0 and v_2 are already obtained in (6.19.2) and (6.19.3). As this process is lengthily we limit ourselves in just describing the procedure. In the following subsection we use the above results to introduce Mathieu´s beams.

6.3 Mathieu´s beams

Mathieu´s beams can be written as

$$\psi(\xi,\eta,z) = \begin{cases} \sum_{m=0}^{\infty} A_m Ce_m(q,\xi)ce_m(q,\eta)e^{\pm ik_z z} & (even) \\ \sum_{m=0}^{\infty} B_m Se_m(q,\xi)se_m(q,\eta)e^{\pm ik_z z} & (odd) \end{cases} , \qquad (6.21)$$

where A_m and B_m are amplitude coefficients, $m = 2n$ or $m = 2n+1$.

In the following figures we plot some Mathieu´s functions.

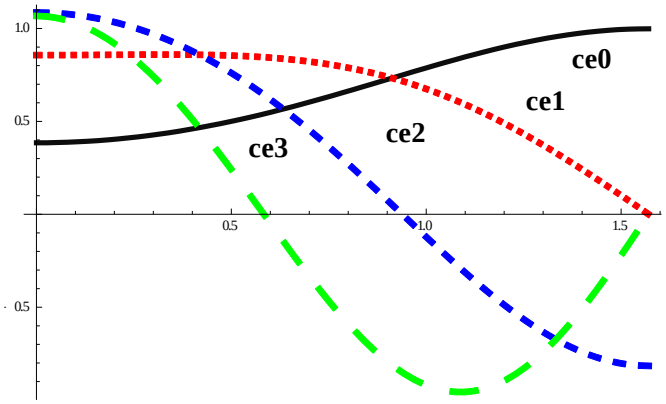

Figure 6.1 Even periodic Mathieu Functions. Orders 0 - 3. $q = 1$

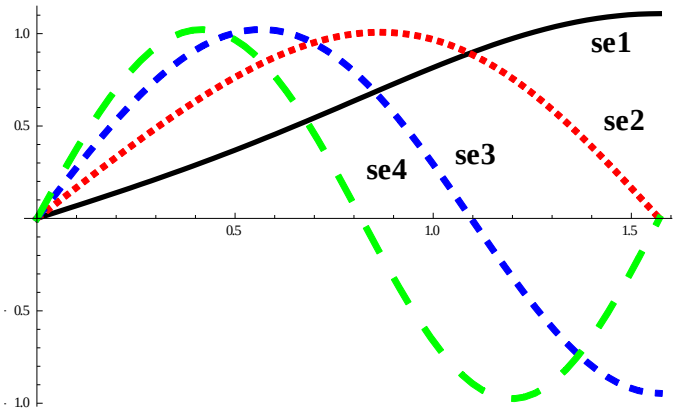

Figure 6.2 Odd periodic Mathieu Functions. Orders 1 - 4. $q = 1$.

From (6.21) for any order m and parameter q, the intensity of even mode Mathieu beams can be written as:

$$I(\xi,\eta,z) = |\psi(\xi,\eta,z)|^2 = |A_m Ce_m(q,\xi)ce_m(q,\eta)|^2 \ . \qquad (6.22)$$

It can be seen from equation (6.22) that the transverse intensity distribution of Mathieu´s beam maintains the same shape as the beam propagates along the z axis. These Mathieu beams have been experimentally demonstrated [36].

The intensity of Mathieu´s beam zero-order is given by,

$$I(\xi,\eta) = |Ce_0(q,\xi)ce_0(q,\eta)|^2 \,, \tag{6.23}$$

in the next figure 3D-plot are shown for $q = 5,\ q = 25\,,\ q = 55.$

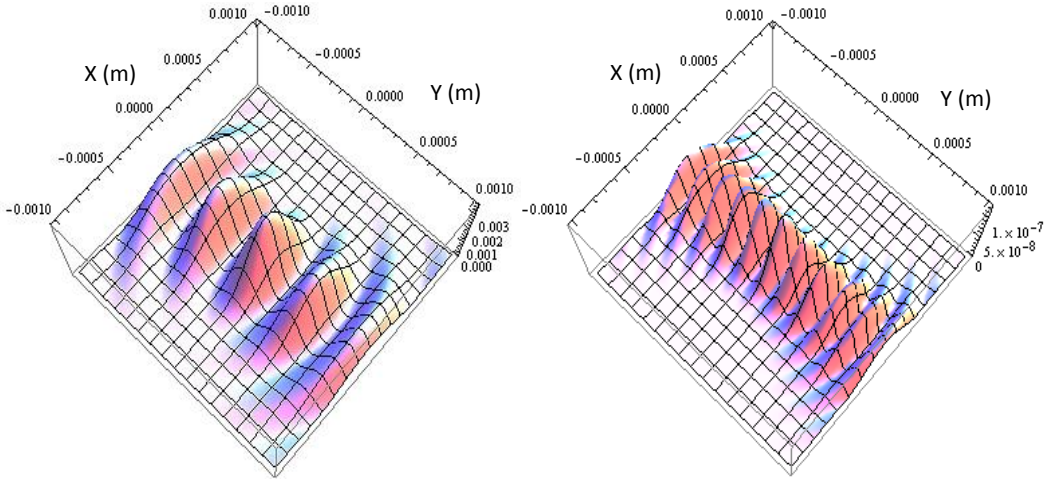

a)

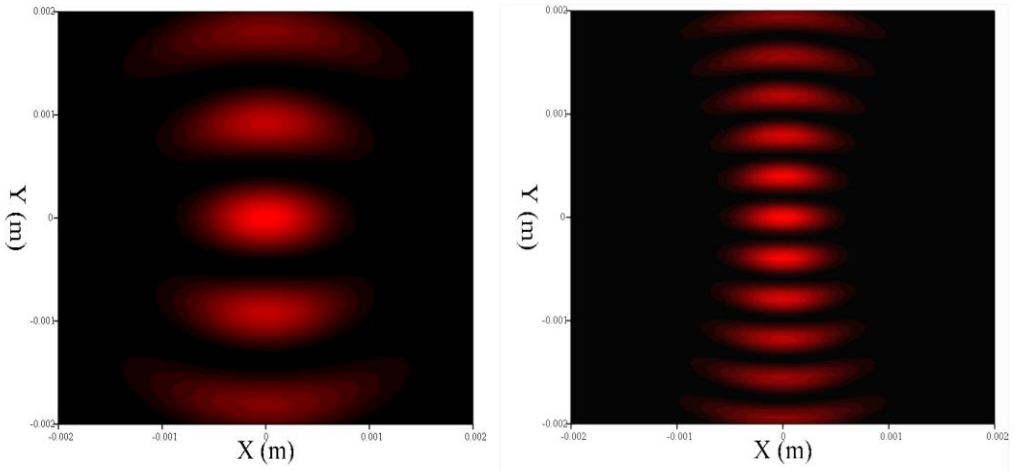

b)

Figure 6.3 a) 3D-Intensity distributions of the even zero-order Mathieu´s beam with parameters $q = 5,\ q = 25\,,$ respectively. b) Contour intensity distributions of the even zero-order Mathieu´s beam with parameters $q = 5,\ q = 25\,,$ respectively.

6.4 The Whittaker integral

The Mathieu´s beam extends without limit; in consequence it also has infinite energy. For their physical realization true beams have to be truncated. Like Bessel beams, this truncation still allows to maintain their non-diffractive properties along reasonable large distances.

To calculate the wave propagation of truncated Mathieu´s beam typically the Whittaker integral is used [36]. In the following we describe a method to obtain the Whittaker.

We begin by writing $\psi(x,y,z)$ as a function of its inverse transform as,

$$\psi(x,y,z) = \iiint_{-\infty}^{\infty} \tilde{\psi}(u,v,\omega) e^{i2\pi(ux+vy+\omega z)} du dv d\omega. \tag{6.24}$$

We will use equation (6.24) to calculate the derivatives involved in the Helmholtz equation,

$$\frac{\partial^2 \psi(x,y,z)}{\partial x^2} = \iiint_{-\infty}^{\infty} (-4\pi^2 u^2) \tilde{\psi}(u,v,\omega) e^{i2\pi(ux+vy+\omega z)} du dv d\omega, \tag{6.25}$$

$$\frac{\partial^2 \psi(x,y,z)}{\partial y^2} = \iiint_{-\infty}^{\infty} (-4\pi^2 v^2) \tilde{\psi}(u,v,\omega) e^{i2\pi(ux+vy+\omega z)} du dv d\omega, \tag{6.26}$$

$$\frac{\partial^2 \psi(x,y,z)}{\partial z^2} = \iiint_{-\infty}^{\infty} (-4\pi^2 \omega^2) \tilde{\psi}(u,v,\omega) e^{i2\pi(ux+vy+\omega z)} du dv d\omega. \tag{6.27}$$

Adding equations (6.25) to (6.27) we obtain

$$[-4\pi^2(u^2+v^2+\omega^2) + k^2]\tilde{\psi}(u,v,\omega) = 0. \tag{6.28}$$

To proceed further we define

$$2\pi u = k_x = K \sin\Theta \sin\Phi, \tag{6.29}$$

$$2\pi v = k_y = K \cos\Theta, \tag{6.30}$$

$$2\pi \omega = k_z = K \sin\Theta \cos\Phi, \tag{6.31}$$

Substituting the above equations into (6.28) we obtain

$$[-K^2 + k^2]\tilde{\psi}(k_x, k_y, k_z) = 0\,. \tag{6.32}$$

Equation (6.32) is written as

$$(K-k)(K+k)\tilde{\psi}(k_x, k_y, k_z) = 0\,, \tag{6.33}$$

From equation (6.33) it is evident that $\tilde{\psi}(k_x, k_y, k_z)$ can be written as

$$\tilde{\psi}(k_x, k_y, k_z) = S(k_x, k_y, k_z)\delta(K - k). \tag{6.34}$$

Substituting (6.34) in equation (6.24) we obtain

$$\psi(x, y, z) = \frac{1}{(2\pi)^3} \iiint S(k_x, k_y, k_z)\delta(K - k)e^{i2\pi(k_x x + k_y y + k_z z)} dk_x dk_y dk_z. \tag{6.35}$$

At this point it is possible to propose several analytical forms for the spectral function.

A simple case can be proposed as

$$S(k_x, k_y, k_z) = S_1(K)S_2(\Theta)S_3(\Phi)\,. \tag{6.36}$$

In spherical coordinates in the spectral space we have

$$dk_x dk_y dk_z = K^2 \sin\Theta d\mathrm{K} d\Phi d\Theta\,, \tag{6.37}$$

then

$$\psi(x, y, z) = \frac{1}{(2\pi)^3} \int_{K=0}^{\infty} \int_{\Theta=0}^{\pi} \int_{\Phi=0}^{2\pi} S_1(K)S_2(\Theta)S_3(\Phi) \cdot \ \delta(K - k) \sin\Theta \cdot e^{iK(x \sin\Theta \sin\Phi + y \cos\Theta + z \sin\Theta \cos\Phi)} K^2 d\mathrm{K} d\Phi d\Theta\,. \tag{6.38}$$

Equation (6.38) readily gives

$$\psi(x, y, z) = \frac{k^2 S_1(k)}{(2\pi)^3} \int_{\Phi=0}^{2\pi} \int_{\Theta=0}^{\pi} S_2(\Theta)S_3(\Phi)\, e^{ik(x \sin\Theta \sin\Phi + y \cos\Theta + z \sin\Theta \cos\Phi)} \sin\Theta d\Theta d\Phi. \tag{6.39}$$

Finally it is customary to propose

$$S_3(\Phi) = e^{im\Phi}\ . \tag{6.40}$$

Thus,

$$\psi(x, y, z) = \frac{k^2 S_1(k)}{(2\pi)^3} \int_{\Phi=0}^{2\pi} \int_{\Theta=0}^{\pi} S_2(\Theta) e^{im\Phi}\, e^{ik(x \sin\Theta \sin\Phi + y \cos\Theta + z \sin\Theta \cos\Phi)} \sin\Theta d\Theta d\Phi. \tag{6.41}$$

Equation (6.41) is the *Whittaker integral* which is obtained by other means in other reports [37].

In a similar way as in previous chapters, $S_2(\Theta)$ represents the main key to obtain different solutions. As we have demonstrated that Mathieu´s functions satisfy the differential wave equation one possibility is to assume that $S_2(\Theta)$ should be Mathieu´s functions. It is customary to use a combination of even - odd functions [38]. For example two typical spectrums are the following,

$$S_2(\Theta) = ce_{2m}(\Theta) + ise_{2m+1}(\Theta)\,, \tag{6.42}$$

and

$$S_2(\Theta) = se_{2m}(\Theta) + ice_{2m+1}(\Theta)\,. \tag{6.43}$$

In figures (6.4.a) and (6.4.b) the real versus the imaginary part of each spectrum are plotted for a particular case, $m = 10$ and $q = 4$.

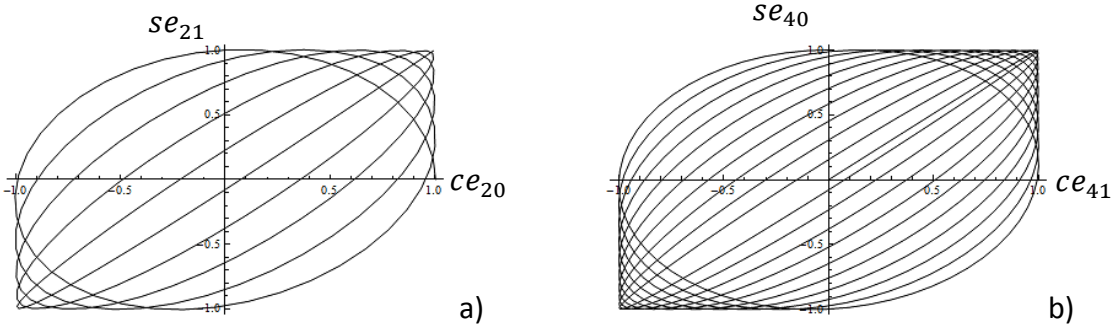

Figure 6.4 a) Angular spectrum function formed with $se_{21}(q,\eta)$ in y-axis and $ce_{20}(q,\eta)$ in x-axis with $q = 4$, b) angular spectrum function formed with $se_{40}(q,\eta)$ in y-axis and $ce_{41}(q,\eta)$ in x-axis with $q = 4$.

Before finishing this chapter we want to remark that $S_2(\Theta)$ has to be inserted in the Whittaker integral, equation (6.41), to calculate the propagation of the beam. The resulting integrals are complex and must be solved numerically; however this subject is out of the scope of this presentation.

Chapter 7

Conclusions

We have described analytical methods for finding solutions to the differential wave equation in free space which, for some cases, yields non-diffractive beams or pulses. For this task we followed two possible approaches. In the first approach we used a Bessel-Fourier expansion in the transversal part of the differential equation. In the second approach we used some analytical form for the transversal part of the equation which by additionally considering that the transversal term of the equation as axisymmetric allows to be solved by Fourier transforming the resulting equation.

With the first approach we have demonstrated that there is a spectral function that results being the main key to yield different solutions. Some of the solutions resulted in non-diffracted pulses or beams. Other of the solutions resulted in well-known diffractive beams. We saw that the choice of their spectral components affect on the propagating characteristics. The non-diffractive depth propagation of a beam can be controlled by varying only their spatial spectral content or changing their energy distribution over the aperture. For example changing the aperture to get more rings in Bessel beams can give us a larger non-diffracting propagation depth than the same Bessel beam with less rings because it changes its spatial spectral function. Then comparing a Gaussian beam with a Bessel beam which have the same semi-width (and identical apertures), we notice that Bessel beam have a larger depth compared to a Gaussian energy distribution.

On the other hand, some spectral functions lead pulses where their temporal and spatial spectral components were important in their limiting propagation characteristics. It has been demonstrated that certain types of pulses are localized X-waves and that reconstruct themselves as they propagate in free space.

With the second approach we have obtained Gaussian localized pulses which we have characterized. This method provides a new approach that could give us some information that may be concealed by formal approaches like the Fourier analysis. This method gives a rich class of possible solutions depending on the election of the function in the Laplace transform (5.41) (with no physical meaning until now). Finally, we have provided a classification of the different results obtained which can found to be useful for future applications.

There is another method to the wave propagation where the Whittaker integral is used. This integral also uses a spectral function but with the difference that this spectral function has angular dependence (in spherical, elliptic or paraboloid coordinates) in difference with the only radial dependence in the Bessel beam (circular symmetry).

For future work further investigation is needed to study the feasibility of the distributions obtained in order to know which solutions may be useful for specific applications and which will be useful only for theoretical foundations.

Bibliography

[1] Lu, Jian-yu, and James F. Greenleaf. "Diffraction-limited beams and their applications for ultrasonic imaging and tissue characterization." San Diego'92, International Society for Optics and Photonics, 1992.

[2] Recami, E. and Zamboni-Rached, M. (2011) Non-diffracting waves, and Frozen Waves: An Introduction, 121 pages online in Geophysical Imaging with Localized Waves.

[3] B. Brittingham: "Focus wave modes in homogeneous Maxwell's equations: Transverse electric mode", *Appl. Phys*., vol 54, no. 3, pp. 1179-1189, 1983.

[4] R. W. Ziolkowski: "Exact solutions of the wave equations with complex source locations," *J. Math Phys*., vol. 26, no. 4, pp. 861463, Apr. 1985.

[5] A. M. Shaarawi, I. M. Besieris, and R. W. Ziolkowski. "Localized energy pulse train launched from an open, semi-infinite, circular waveguide", *J. Appl Phys*., vol. *65,* no. 2, pp. 80S13, 1989.

[6] E. Heyman, B. Z. Steinberg, and L. B. Folsen, "Spectral analysis of focus wave modes", *J. Opt. Soc. Amer. A,* vol. 4, *no.* 11, pp. 2081-2091, 1987.

[7] J, Durnin, "Exact solutions for non-diffracting beams: The scalar theory", *J. Opt. Soc*.. vol. 4, no. 4, pp. 651-654. 1987.

[8] K. Uehara and H. Kikuchi, "Generation of near diffraction-free laser beams." *Appl. Physics B,* vol. 48, pp. 125-129, 1989.

[9] Jian-yu Lu and J.F. Greenleaf: "Non-diffracting X waves - exact solutions to free space scalar wave equation and their finite aperture realizations", *IEEE Trans. Ultrason. Ferroelec., Freq. Contr.*, vol 39, no. 1, 1992.

[10] R. W. Ziolkowski,D. K. Lewis, and B. D. Cook: "Evidence of localized wave transmission," *Phys.Rev. Lett*., vol. 62, no. 2, pp. 147-150, Jan.9, 1989.

[11] Lu, Jian-yu, and James F. Greenleaf, "Experimental verification of nondiffracting X waves." Ultrasonics, Ferroelectrics, and Frequency Control, IEEE Transactions on 39.3 (1992): 441-446.

[12] P. Saari and K. Reivelt, ``Evidence of X-shaped propagation-invariant localized light waves,'' Phys. Rev. Lett. 79, 41354138 , 1997.

[13] Ziolkowski, Richard W., Ioannis M. Besieris, and Amr M. Shaarawi, "Aperture realizations of exact solutions to homogeneous-wave equations." JOSA A 10.1 (1993): 75-87.

[14] Remoissenet, Michel. "Waves called solitons: concepts and experiments". Springer Science & Business Media, chapter 1, 2013.

[15] A. Sezginer: "A general formulation of focus wave modes", J. App. Phys., vol. 57, pp. 678, 1985.

[16] J, Durnin. J. J. Miceli. Jr., and J. H. Eberly, "Diffraction-free beams." *Phys. Rev., Lett.,* vol. *58,* no. 15, pp. 1499-1501. Apr. 13. 1987.

[17] J, Durnin, J.J.Miceli and J.H.Eberly: "Comparison of Bessel and Gaussian beams", *Optics Letters*, vol.13, pp.79-80, 1988.

[18] L. Vicari. "Truncation of non-diffracting beams. " *Optics Commun*., vol 70, no. 4, pp. 263-266, Mar. 15 1989.

[19] M. Zahid and M. S. Zuhairy, "Directionally of partially coherent Bessel-Gauss beams," *Optics Commun* vol. 70, no. 5, pp. 361-364. Apr. *1,* 1989.

[20] P.L.Overfelt and C.S.Kenney: "Comparison of the propagation characteristics of Bessel, Bessel-Gauss, and gaussian beams diffracted by a circular aperture", *Journal of the Optical Society of America A*, vol.8, pp.732-745 , 1991.

[21] Cox A J and Dibble D C, "Nondiffracting beams from a spatially filtered Fabry–Perot resonator" *J. Opt. Soc.Am.* A 9 282–6, 1992.

[22] Horvath Z L, Erdelyi M, Szabo G, Bor Zs, Tittel F K and Cavallaro J R 1997 "Generation of nearly nondiffracting Bessel beams with a Fabry–Perot interferometer", *J. Opt. Soc. Am.* A 14 3009–13

[23] Herman R M and Wiggins: "Production and uses of diffractionless beams", *J. Opt. Soc. Am.* A 8 932–42, 1991.

[24] Armito R, Saloma C, Tanaka T and Kawata S: "Imaging properties of axicons in a scanning optical system", *Appl. Opt.* 31 6653–7, 1992.

[25] Vahimaa P, Kettunen V, Kuittinen M, Turunen J and Friberg: "Electromagnetic analysis of nonparaxial Bessel beams generated by diffractive axicons", *J. Opt. Soc. Am.* A 14 1817–24, 1997.

[26] Hsu D K, Margetan F J and Thompson: "Bessel beam ultrasonic transducer: Fabrication method and experimental results", *Appl. Phys. Lett.* 55 2066–8, D O 1989.

[27] Zamboni-Rached, Michel, and Erasmo Recami. "Acoustic (Ultrasonic) Non-Diffracting Beams: Some theory, and Proposals of Acoustic Antennas for several purposes." arXiv preprint: 1411.3340 (2014).

[28] Goodman, Joseph W., "Introduction to Fourier optics". Roberts and Company Publishers, Chapter 4, 2005.

[29] Iizuka, Keigo ; Rhodes,William T., "Engineering optics". Springer Science & Business Media, Chapter 2, 2013.

[30] George O Reynolds; John B DeVelis; George B Parrent Jr; Brian J Thompson, "The New Physical Optics Notebook: Tutorials in Fourier Optics", chapter 1,2,9, 1989.

[31] Arfken, George B., Hans J. Weber, and Frank E. Harris., "Mathematical methods for physicists: A comprehensive guide". Academic press, 2011.

[32] Hernández-Figueroa, H. E., Zamboni-Rached, M., & Recami, E., "Localized waves", Vol. 194, John Wiley & Sons, pp. 243, 2007.

[33] Recami, Erasmo, "Superluminal motions? A bird's-eye view of the experimental situation." Foundations of Physics 31.7: 1119-1135, 2001.

[34] Mugnai, D., A. Ranfagni, and R. Ruggeri, "Observation of superluminal behaviors in wave propagation." Physical review letters 84.21: 4830, 2000.

[35] M. Abramowitz and I. Stegun, "Handbook of Mathematical Functions" (Dover, N.Y. 1964), Chapter 20.

[36] Gutiérrez-Vega, J. C., et al. "Experimental demonstration of optical Mathieu beams." *Optics Communications* 195.1 (2001): 35-40.

[37] E. T. Whittaker and G. N. Watson, "A Course of Modern Analysis", (4th ed. Cambridge University Press, Westford, MA, 1927), Chapter 19.

[38] Zhang, Yiqi, et al. "Three-dimensional nonparaxial accelerating beams from the transverse Whittaker integral." *EPL (Europhysics Letters)* 107.3 (2014): 34001.